

DR 20585-1

## SIGNS OF NEW W'S AND Z'S\*

HOWARD E. HABER

Department of Physics, University of California, Santa Cruz, CA 95064  
and

Stanford Linear Accelerator Center, Stanford University, Stanford, CA 94305

30/11-15-84 WF. (1)

This report reflects the collective efforts of the New W/Z Physics Subgroup. The active members of the group included Carl Albright, Sam Aronson, Nilendra Deshpande, Fred Gilman, Jack Gunion, Howard Haber, Boris Kuyser, Tom O'Halloran, Bernard Pope and George Tsanakos.

## Summary

If new heavy charged and/or neutral gauge bosons exist with masses below 5 to 10 TeV, they can be observed at the SSC. In this report, we summarize the work of the New W/Z Physics Subgroup. The expected properties of new heavy gauge bosons (such as new W's and Z's or horizontal gauge bosons) are summarized. We then discuss various signatures of these new gauge bosons and their implications for detector designers. Suggestions for future work are indicated.

## 1. Introduction

## A. Scope of this Report

The plan of this report is as follows. First we present in Section 1 a general introduction to the subject of new W's and Z's - motivation, current mass limits, and a brief survey of models. In Section 2, we review the results known before the Snowmass meeting which formed the basis for our group's work. One piece of work of particular value for our group was a paper by Langacker, Robinett and Rosner<sup>1,2</sup> (henceforth to be called LRR). Many of their results are summarized in section 2B and 2C. The remainder of the report summarizes the collective efforts of our group members. In Section 3, we consider potential impact of the physics of new W's and Z's on the design of SSC detectors. The main focus is on leptonic decays of new W's and Z's. It was found that the requirement that electrons and muons of  $p_T \gtrsim 1$  TeV be detected (with sign determination) in the same apparatus leads to very large yet precise detectors. In Section 4, theoretical aspects of new W and Z physics relevant to the SSC are discussed. Topics include: (a) discovery limits of new W's and Z's in  $p\bar{p}$  vs.  $e^+e^-$  colliders, (b) asymmetries, (c) the importance of seeing  $\tau$  leptons arising from new W and Z decays, (d) horizontal gauge bosons, and (e) implications of a new neutral heavy lepton. We end with a list of suggestions for future work.

## B. Motivations for Searching for New Heavy Gauge Bosons

The Standard Model postulates that the appropriate electroweak gauge group is  $SU(2) \times U(1)$ . Combining this work with QCD based on color  $SU(3)$ , one arrives at  $SU(3) \times SU(2) \times U(1)$  as the appropriate gauge theory which at present describes observed particle physics phenomena. The crucial feature of this theory is electroweak symmetry breaking which is responsible for giving mass to the  $W^\pm$  and  $Z^0$  gauge bosons while leaving the photon massless. The recent observation of the  $W(83)$  and the  $Z(94)$ <sup>3</sup> at the CERN Collider<sup>4</sup> has been one further confirmation of the Standard Model approach.

\* Work supported in part by the National Science Foundation, grant PHY8115541 and by the Department of Energy, contract DE-AC03-76SF00515.

The large mass of the  $W(83)$  and  $Z(94)$  reflect the large scale of electroweak symmetry breaking. In the Standard Model, this scale corresponds to the fact that an elementary scalar Higgs field acquires vacuum expectation value  $v = (\sqrt{2}G_F)^{-1/2} \approx 250$  GeV. The Higgs boson sector of the theory is the least well understood part of the Standard Model; in particular, the reason for the size of the electroweak scale of 250 GeV is a mystery. Many attempts to gain insight into the mechanism of electroweak symmetry breaking have been made, often resulting in the prediction of new physical phenomena<sup>5</sup> at a scale on the order of (or not much larger than) 250 GeV. This is the main theoretical motivation for building the SSC.<sup>6</sup>

Attempts have also been made to incorporate the  $SU(3) \times SU(2) \times U(1)$  theory into a larger framework. For example, in the grand unification approach,<sup>7</sup>  $SU(3) \times SU(2) \times U(1)$  is viewed as a "low energy" effective theory to be replaced at a superheavy mass scale of order  $10^{15}$  GeV by a gauge theory based on a unifying simple gauge group such as  $SU(5)$ . However, our goals are much more modest at the SSC. Here, we can simply ask whether the  $SU(3) \times SU(2) \times U(1)$  theory needs to be embedded in a larger gauge group to explain phenomena at the 1 TeV scale. For simplicity, we assume that  $SU(3)$  color will be unmodified by such an extension. It is useful to review the theoretical motivations for considering an electroweak gauge group larger than  $SU(2) \times U(1)$ .

1. The Empirical Approach. We do not know why the electroweak gauge group which describes present day phenomena is  $SU(2) \times U(1)$  as opposed to some other gauge group. We have no physical principle which allows us to deduce the number of physical gauge bosons.

2. Parity Invariance. The  $SU(2) \times U(1)$  model does not explain parity violation - it is put in by hand. One can construct models left-right symmetric theories<sup>8-10</sup> based on  $SU(2)_L \times SU(2)_R \times U(1)$  in which parity invariance is respected by the Lagrangian but is spontaneously broken by some Higgs field vacuum expectation value.

The fermions of each generation transform under the  $SU(2)_L \times SU(2)_R \times U(1)$  group as follows:

$$\begin{pmatrix} u_L \\ d_L \end{pmatrix}, \begin{pmatrix} \nu_L \\ e_L \end{pmatrix} \quad J_L = \frac{1}{2}, \quad J_R = 0 \quad (1.1a)$$

$$\begin{pmatrix} u_R \\ d_R \end{pmatrix}, \begin{pmatrix} \nu_R \\ e_R \end{pmatrix} \quad J_L = 0, \quad J_R = \frac{1}{2} \quad (1.1b)$$

Note that we must necessarily add a new field, the  $N_R$ . This may or may not be related to the  $\nu_R$  as we shall discuss shortly. As for the gauge bosons, we identify the  $W_L^\pm$  gauge bosons with the usual  $W(83)$  and predict the existence of new  $W_R^\pm$  bosons and an additional new neutral gauge boson. The suppression of right-handed charged currents in low energy phenomena is then explained by the smallness of the parameter  $M_{W_R}^2/M_{W_L}^2$ . The  $U(1)$  symmetry in this model corresponds to  $B - \bar{L}$ .

Presented at the 1984 Summer Study on the Design and Utilization of the Superconducting Super Collider, Snowmass, Colorado, June 23 - July 13, 1984.

**3. Neutrino Masses.** In the  $SU(2) \times U(1)$  model, neutrinos are exactly massless. This occurs for two reasons. First, no  $\nu_R$  field is introduced to the theory; this forbids a Dirac mass for the neutrino. Second, there exists no Higgs fields which couples  $\nu_L$  to itself. As a result, no Majorana mass term for  $\nu_L$  can develop.<sup>11</sup> Clearly, this construction is artificial. It turns out that neutrinos do have very small but non-zero masses; it will be difficult to explain the origin of such a small number in the  $SU(2) \times U(1)$  framework. In  $SU(3)_L \times SU(2)_R \times U(1)$  models, there is a "natural" explanation for small neutrino masses. These models contain both a  $\nu_L$  and a  $\nu_R$  field. The general form for the neutrino mass matrix is:

$$\mathcal{L}_{\text{mass}} = m_D (\nu_L \nu_R + \text{h.c.}) + m_L \nu_L^\dagger C^{-1} \nu_L + m_R \nu_R^\dagger C^{-1} \nu_R \quad (1.2)$$

It is natural to expect  $m_D$  to be of order a lepton mass (say  $m_D = m_e$  for  $\nu_e$ ). By appropriate choice of the Higgs boson sector of the theory, one can arrange  $m_L = 0$  and  $m_R$  to be large (of order the  $SU(2)_R$  breaking scale). In this limit, one finds<sup>12</sup> two Majorana neutrinos of mass  $m_R$  and  $m_R^3/m_D$ . The latter neutrino is identified with the presently observed neutrino. We see that if  $m_D \ll m_R$ , one obtains a very light neutrino which is compatible with present observations. An important consequence is the existence of a neutral heavy Majorana neutrino which may be observable at the SSC. Unfortunately, in the context of model building, there is no precise prediction for the value of such a heavy neutrino.<sup>13</sup> It could be as light as a few GeV; alternatively, it may be much heavier. We shall have more to say about this neutral heavy lepton in Section 4E.

**4. CP - violation.** There is no fundamental understanding as to the origins of CP-violation as observed in the neutral kaon sector. One can parameterize the CP-violation as being due to a complex phase in the Cabibbo-Kobayashi-Maskawa (CKM) mass matrix.<sup>14</sup> However, based on recent measurements of the  $\epsilon$  and  $\epsilon'$  parameters<sup>15</sup> and the b-quark lifetime,<sup>16</sup> there have been hints that the Standard Model may be incapable in explaining the observed data. In some left-right models, the major contribution to the  $\epsilon$  parameter is due to the presence of right-handed currents (specifically, CP-violation is arising in part due to a relative phase between the left-handed and right-handed CKM matrices). One predicts<sup>17,18</sup>  $\epsilon$  to be of order  $M_{W_R}^2/M_{W_L}^2$ ; this allows one to deduce (in principle) an upper limit to the scale of left-right symmetry breaking! Recently, Harari and Leurer<sup>17</sup> have argued that the  $W_R$  mass based on the above arguments should be about 10 TeV (within a factor of two). Such a mass range is partly accessible to the SSC.

**5. Grand Unification.** The Standard Model may be embedded in a grand unification gauge group; the minimal model is based on  $SU(5)$ . This model also has parity violation and a massless neutrino for the same reasons as discussed above. In addition, this model predicts a "desert," i.e. no new physical phenomena between the  $W(83)$  and  $Z(94)$  and the grand unification mass (of order  $10^{14}$  GeV). The grand unification mass is one of the predictions of the model; it may be computed based on the knowledge of "low energy" physics (the values of the various coupling constants and particle masses). This mass is then used to predict the rate for proton decay; it is well known that the proton lifetime as measured is significantly longer than the minimal  $SU(5)$  prediction.<sup>19</sup>

A reasonable interpretation of this result is that the "desert" hypothesis is wrong, and new physical phenomena will appear

beyond 100 GeV. In the context of grand unification, the simplest possibility is to consider a larger gauge group such as  $SO(10)$ . It is possible to embed left-right symmetric models such as  $SU(3) \times SU(2)_L \times SU(2)_R \times U(1)$  in  $SO(10)$ , although it is not obvious where the  $SU(2)_R$  breaking scale should be. Many attempts to construct such models with light  $SU(2)_R$  breaking scales have been made.<sup>20</sup> We shall not go into details of model building here. However, it is useful to point out that the algebraic structure of such models<sup>1</sup> is interesting to study independent of the details of the dynamics. Such a study can yield information on how new heavy  $Z^0$ -bosons can couple to quarks and leptons. Such information is needed in order to predict production rates and decay properties of new hypothetical  $Z^0$ -bosons which could be seen at the SSC.

#### B. Current Mass Limits on New W's and Z's

If new W's and Z's exist, they must either be more massive than the  $W(83)$  and  $Z(94)$  or else very weakly coupled to known quarks and leptons. One minor complication arises due to the possibility of mixing: e.g., in  $SU(2)_L \times SU(2)_R \times U(1)$  models, the physical charged gauge bosons can be a mixture of  $W_L$  and  $W_R$ . In this regard, Langacker<sup>21</sup> has made the following observation. We already know that the  $W(83)$  and  $Z(94)$  as observed at the CERN Collider are quite close in mass to the values predicted by the  $SU(2) \times U(1)$  electroweak model. As a result, Langacker shows<sup>22</sup> that under a few reasonable assumptions, the mixing of the  $W(83)$  and  $Z(94)$  with hypothetical heavier W's and Z's is suppressed proportional to the inverse mass squared of the new vector bosons. For example, if the  $W(83)$  and  $Z(94)$  masses were found to be within 1 GeV of their predicted  $SU(2) \times U(1)$  values, then the mixing angles to any new vector boson with mass of 200, 500, or 1000 GeV would be bounded by 0.07, 0.03 and 0.01 respectively. Henceforth, we shall ignore the possibility of such mixing.

In order to be more precise about mass limits for new W's and Z's, one has to use the framework of some electroweak gauge group beyond  $SU(2) \times U(1)$ . Let us consider the limits one obtains in the context of an  $SU(2)_L \times SU(2)_R \times U(1)$  model. Even within this context, one gets different bounds depending on various model assumptions made. We give a sample of the bounds<sup>17,21-28</sup> obtained in Table I for the mass of a  $W_R$  which has right-handed couplings to all fermions. For an experimentalist designing new W' searches, the relevant bound is  $M_{W_R} \gtrsim 300$  GeV. The theorist's favorite bound is  $M_{W_R} \gtrsim 1-2$  TeV which arises in two popular versions of  $SU(2)_L \times SU(2)_R \times U(1)$ . In one version ("manifest left-right symmetry"), the left and right handed CKM angles are assumed to be equal. In a second version ("pseudomanifest left-right symmetry" or "charge conjugation conserving"), the Lagrangian conserves separately C, P and T; these discrete symmetries are spontaneously broken. In the latter case, the magnitude of CP-violation is related to the scale of  $SU(2)_R$  breaking as mentioned in the last sub-section.

Bounds for new  $Z^0$  masses are even more model-dependent. Unlike in the case of a  $W_R$ , the  $Z^0 f \bar{f}$  interaction is a model-dependent mixture of  $V - A$  and  $V + A$ . Furthermore, the interpretation of  $\sin^2 \theta_W$  as determined from the neutral current data may be changed.<sup>20</sup> It is probably safe to conclude that for a new Z,  $M_Z \gtrsim 150$  GeV. A more precise estimate can only be made in the context of a particular model.

Table 1

$(M_{W_R})_{\min}$	Process	Assumption	Ref.
300 GeV	$K_L^0 - K_S^0$ mass difference and $b$ -quark decay	none	21
300 GeV	nonleptonic decays	manifest $L$ - $R$ symmetry	22
380 GeV	$\mu$ and $\beta$ decay	light Dirac $\nu$	23, 24
1-2 TeV	$K_L^0 - K_S^0$ mass difference and $b$ -quark decay	manifest $L$ - $R$ symmetry or charge con- jugation con- serving	25, 26, 17
2 TeV	$\pi^- \rightarrow e_R^- \nu_R$	light Majorana $\nu$	27, 28

Table 1: Lower bound on the  $W_R$  mass in  $SU(2)_L \times SU(2)_R \times U(1)$  under the assumptions stated above.C. Basic Properties of New  $W$ 's and  $Z$ 's

We have argued that a new  $W$  would probably exhibit negligible mixing with the  $W(83)$ . Thus, in  $SU(2)_L \times SU(2)_R \times U(1)$  models, a heavier  $W$  would have pure  $V + A$  couplings to quarks and leptons. It is also natural to assume that the gauge couplings of the  $SU(2)_L$  and  $SU(2)_R$  groups are equal. The only remaining question is the nature of the  $W_R$  couplings to charged leptons. We have two choices - (a) we can take the neutrino to be a Dirac fermion or (b) we can assume that there are two Majorana neutrinos:  $\nu$  and  $N$ . In the former case,  $W_R^+ \rightarrow e^+ \nu$  where  $\nu$  is the right-handed component of the ordinary neutrino. In the latter case,  $W_R^+ \rightarrow e^+ N$  where  $N$  is a new neutral lepton. The signature of new  $W$ 's in the latter case then depends on whether the decays of the  $N$  are observable. The  $W_R$  decay widths and branching ratios are easily obtained:

$$BR(W_R^+ \rightarrow e^+ N_f) = \frac{1}{4N_G} \quad (1.3a)$$

$$BR(W_R^+ \rightarrow \bar{u}d) = \frac{3}{4N_G} \quad (1.3b)$$

$$\Gamma(W_R) = \frac{M_{W_R}}{M_W} \Gamma(W) \quad (1.3c)$$

where  $M_W$  and  $\Gamma(W)$  are the mass and width of the  $W(83)$  and  $N_G$  is the number of generations of fermions. Occasionally, we may wish to be less tied to particular electroweak gauge model. It will then be of interest to explore the consequence of a new  $W$  with pure  $V - A$  or pure  $V$  interactions.

A new  $Z$  would decay into fermion pairs with model-dependent couplings. Consider the following three models:

- A new heavy  $Z$  with couplings to fermions which are identical to those of the  $Z(94)$ . This model is artificial but useful in making comparisons with  $Z(94)$  production rates. See Table 2.
- In  $SO(10)$  grand unified models, each fermion belongs to a single 16 dimensional representation which decomposes under  $SU(5)$  into a 5 ( $d^c, e, \nu$ ), a 10 ( $d, u, e^c, e^c$ ) and a 1 ( $N^c$ ). All particles listed are left-handed; charge conjugates are indicated by a  $\bar{c}$ . Such models contain a new

$Z$  which couples to a new hypercharge  $x$  which depends solely on which  $SU(5)$  multiplet the fermion lives in. The (unnormalised) values of the hypercharge  $x$  are 1, -3 and 5 for the 10, 5 and 1 respectively. The relative branching ratios are easily obtained. For example, the coupling of  $Z$  to  $e^c \bar{e}$  is  $j^0 Z_p$ , where<sup>20</sup>

$$\begin{aligned} j^0 &= \bar{e}_L \gamma^{\mu} e_L - 3 \bar{e}_L^c \gamma^{\mu} e_L^c \\ &= \bar{e}_L \gamma^{\mu} e_L + 3 \bar{e}_R \gamma^{\mu} e_R \\ &= \bar{e} \gamma^{\mu} (g_V + g_A T_3) e \end{aligned} \quad (1.4)$$

where  $g_V = 2$  and  $g_A = 1$ . Thus,  $BR(Z \rightarrow dd)$  is proportional to  $3(g_V^2 + g_A^2)$  where the factor of 3 is required for the color triplet  $d$ -quark. We denote this  $Z$  by  $Z_q$ ; its relative couplings to fermions obtained in a similar manner as above are displayed in Table 2.

- The new  $Z$  could couple uniformly to all fermions in the 16 dimensional representation. We denote this neutral boson by  $Z_q$ . It couples to  $j^0 = \bar{f}_L \gamma^{\mu} f_L + \bar{f}_L^c \gamma^{\mu} f_L^c = -\bar{f} \gamma^{\mu} f$  (cf. eq. 1.4), i.e. its couplings are purely axial. The relative decay rates are displayed in Table 2.

Table 2

Fermion pair	Relative couplings to $J/\psi$		
	$g^0$	$Z_q^0$	$Z_q^0$
$e^+ e^-$	$2s_W^0 - s_W^0 + \frac{1}{3}$	10	2
$\nu D$	$\frac{1}{3}$	9	1
$N \bar{N}$	0	25	1
$u \bar{u}$	$\frac{1}{3}s_W^0 - 2s_W^0 + \frac{1}{3}$	6	6
$d \bar{d}$	$\frac{1}{3}s_W^0 - 2s_W^0 + \frac{1}{3}$	30	6
Normalization	$(\frac{1}{3}s_W^0 - 4s_W^0 + 2) N_G$	$80N_G$	$16N_G$

Table 2: The branching ratio for  $Z^0 \rightarrow J/\psi$  is obtained by dividing the relative couplings by the Normalisation factor listed above. The number of generations is denoted by  $N_G$ , and  $s_W = \sin \theta_W$ . For more details, see ref. 1.

Note that we have assumed that the  $Z_q$  and  $Z_q^0$  do not mix<sup>20</sup> with the  $Z(94)$ ; hence their couplings to fermions are independent of  $\sin^2 \theta_W$ . The total width of the new  $Z$  depends on the coupling constant which corresponds to the new hypercharge. In a particular grand unification model, this coupling would be determined by the unification condition. Typically, it is of order the weak coupling constant  $g_W$ . Thus, the total width of a new  $Z$  would be expected to be given by a formula analogous to eq. 1.3(c).

## D. Other New Gauge Bosons

Up until now, we have restricted our discussion to gauge bosons which arise from a simple enlargement of the electroweak gauge group. The resulting gauge bosons had universal couplings to each generation (up to some possible new unknown CKM-type mixing angles). One can discuss gauge bosons which do distinguish among generations. This can occur for example in models which possess a horizontal gauge symmetry.<sup>31,32</sup> In such cases, fermions carry a horizontal quantum number which distinguishes the different generations.

The most interesting kind of gauge boson of this type is one that mediates flavor changing neutral currents (FCNC's). For example, a gauge boson which coupled to  $d\bar{s}$  and  $e^+ \mu^-$  would

mediate the process  $K_L^0 \rightarrow e^+ \mu^-$  and  $K^+ \rightarrow \pi^+ e^+ \mu^-$  at tree level. These two processes have not been observed (the Particle Data Group<sup>23</sup> listing is  $BR(K_L \rightarrow e\mu) < 6 \times 10^{-6}$  and  $BR(K^+ \rightarrow \pi^+ e\mu) < (5 - 7) \times 10^{-3}$ ) which indicate that the mass of the mediating gauge boson must lie in the multi-TeV range. The precise lower mass limit to such bosons depends on an unknown gauge coupling constant and unknown mixing angles. However, these same factors appear in the computation of production cross sections so that one can get useful bounds on their observability at the SSC. In addition, FCNC's involving third generation fermions are not severely constrained. So, in principle, it is possible for gauge bosons which mediate such FCNC's to be light enough to be accessible at the SSC.

Other schemes exist which lead to new gauge bosons which do not couple universally to the various generations of fermions. One such example is an extended technicolor<sup>24</sup> (ETC) scheme discussed by Holdom.<sup>25</sup> In his model, there are two types of ETC gauge bosons. The first type of ETC gauge bosons is the "usual" technicolor non-singlet boson which couples quarks to techniquarks. The exchange of these bosons leads to the generation of quark masses; which in turn implies that these ETC gauge bosons must have masses of order 10 - 100 TeV. The second type of ETC gauge boson is a technicolor singlet boson which couples quarks to themselves and techniquarks to themselves. The masses of these bosons are not so restricted; in fact, one can imagine the existence of a technicolor singlet gauge boson with mass of order a TeV. In Holdom's model, the lightest technicolor singlet gauge boson couples only to the heavy fermion generations. This is another example of a gauge boson which can distinguish among generations. In this particular case, the dominant decays of such a boson would be into  $t\bar{t}$ ,  $b\bar{b}$ ,  $\tau^+\tau^-$  and pairs of techniquarks which presumably manifest themselves as pairs of  $W$ 's and  $Z$ 's. Such a decay pattern is very similar to that of a heavy Higgs boson, so it is worth considering how the two could be distinguished.

In summary, the origin of generations remains one of the major mysteries of the Standard Model. It is quite possible that the solution to the generation mystery involves physics on the TeV scale which could be accessible at the SSC. The detection of new gauge bosons which are sensitive to the generation quantum numbers could provide a crucial piece in the solution of the generation puzzle.

## 2. New $W$ 's and $Z$ 's - The Basics

### A. Formalism for Calculation of Cross Sections

The parton model may be used to estimate the size of production cross sections of new  $W$ 's and  $Z$ 's at the SSC. The calculation involves a number of simplifying assumptions. First, we compute only the tree level process:  $q\bar{q} \rightarrow W$  or  $Z$ . Second, initial state gluon radiation by the quarks and intrinsic transverse momentum of the annihilating quarks relative to proton beams are neglected. In this approximation, the  $W$  or  $Z$  is produced moving longitudinally to the beam. Third, higher order QCD contributions are neglected. In particular, the "K-factor" which renormalizes the parton model result by an overall factor (roughly,  $K \approx 2$  at the CERN Collider) has been set equal to one. Fourth, the effects of spectators (higher-twist effects) are neglected. We can expect these approximations to yield results which are accurate roughly to within a factor of three.

Under the assumptions stated above, it follows that the production cross section for  $A + B \rightarrow W + X$  is<sup>26</sup>

$$\frac{d\sigma}{dy_W} = \frac{4\pi^2 z_1 z_2}{3m_W^3} \sum_{ij} f_i^{(A)}(z_1, m_W^2) f_j^{(B)}(z_2, m_W^2) \Gamma_{ij} \quad (2.1)$$

where

$$m_W^2 = z_1 z_2 s \quad (2.2a)$$

$$z_1 = \frac{m_W}{\sqrt{s}} e^{y_W} \quad (2.2b)$$

$$z_2 = \frac{m_W}{\sqrt{s}} e^{-y_W} \quad (2.2c)$$

$$\Gamma_{ij} = \Gamma(W \rightarrow ij) \quad (2.2d)$$

$\Gamma_{ij}$  is the partial width of the decay of the  $W$  into partons  $i + j$ . In our numerical work, we shall employ EHLQ structure functions<sup>6</sup> for the  $f_i$ . The rapidity of the  $W$  is obtained from  $E_W = m_W \cosh y_W$  which is equivalent to:

$$y_W = \pm \log \left( \frac{E_W - \sqrt{E_W^2 - m_W^2}}{m_W} \right) \quad (2.3)$$

where we have assumed that the  $W$  is emitted longitudinally along the beam direction. The choice of sign in eq. 2.3 depends on whether the  $W$  is emitted along  $A$  or  $B$ .

In the above discussion, " $W$ " has been used to denote any vector boson. First, suppose that " $W$ " is a neutral vector boson,  $Z$ , which decays into a pair of leptons  $e^+e^-$  or  $\mu^+\mu^-$ . Then by measuring the outgoing lepton energies and their angles with respect to the beam, one can reconstruct uniquely the  $Z$  mass and energy thereby obtaining its rapidity  $y_W$ . However, if " $W$ " is a charged vector boson  $W^\pm$ , the situation is more complicated. If  $W \rightarrow eN$  (or  $W \rightarrow \mu N$ ) where  $N$  is a neutral heavy lepton which decays with no missing energy, then one can reconstruct the  $W$  four-momentum as before. On the other hand, if the  $N$  escapes detection, one does not have a unique determination of the  $W$  kinematics. One can obtain useful information assuming that the total transverse momentum in the event can be reliably measured. Let  $E_e$  and  $\theta_e$  be the electron energy and angle with respect to the beam respectively, as measured in the laboratory. Then by momentum and energy conservation, we can compute the  $N$  momentum and energy:

$$p_N^N = -E_e \sin \theta_e \quad (2.4)$$

$$p_N^N = m_N \sinh y_W - E_e \cos \theta_e \quad (2.5)$$

$$E_N^N = m_N \cosh y_W - E_e \quad (2.6)$$

If we now impose the condition that  $N$  has mass  $m_N$ , we find:

$$\cosh y_W - \sinh y_W \cos \theta_e = \frac{m_N^2 - m_W^2}{2E_e m_N} \quad (2.7)$$

Assuming that  $m_N \ll m_W$ , we can neglect the effect of the  $N$  mass. Then, using  $\cosh y = (1 + \sinh^2 y)^{1/2}$ , we obtain a quadratic equation for  $\sinh y_W$ . Thus, we have a two-fold ambiguity in determining  $y_W$ . (In certain instances, one of the

solutions corresponds to an unphysical value of  $p_T^W$  thereby resolving the ambiguity.) This ambiguity can be problematical if one wants to compare experimental data to theoretical  $y_W$  distributions. A straightforward way to overcome this difficulty is to define a new variable  $\tilde{y}_W$  which is equal to the  $y_W$  corresponding to the solution to eq. 2.7 which minimizes  $|p_T^W|$  given by eq. 2.5.<sup>37</sup> One can then obtain theoretical distributions in  $\tilde{y}_W$  (using Monte Carlo techniques) which can be directly compared to the data.

In the case of charged  $W$  production, it would be more useful to study directly the distributions of the observed electron (or muon). The relevant parton model formula is easily generalized:

$$E_t \frac{d^3\sigma}{dp_T^2} = \frac{1}{2\pi} \sum_{ij} \int dz_1 dz_2 f_i^{(A)}(z_1, m_W^2) f_j^{(B)}(z_2, m_W^2) \frac{1}{E_t} \frac{d\delta^{A+B} - R^{A+B} + X}{dE_t d\cos\theta_e} \quad (2.8)$$

where "unbatted" variables are those measured in the laboratory (i.e., the  $A+B$  center of mass frame) and the "batted" variables are defined in the parton center of mass frame: the electron energy  $E_t$  and the angle  $\theta_e$  between parton  $i$  and the electron. These variables are easily expressed in terms of the momentum fractions  $z_1, z_2$  and the laboratory variables as follow:

$$E_t = p_T \cosh(y - y_W) \quad (2.9)$$

$$\cos\theta_e = \tanh(y - y_W) \quad (2.10)$$

where  $y_W = \frac{1}{2} \log(z_1/z_2)$  and  $y$  and  $p_T$  refer to the electron as measured in the laboratory:

$$p_T = E_t \sin\theta_e \quad (2.11)$$

$$y = -\log \tan\left(\frac{\theta_e}{2}\right) \quad (2.12)$$

We have set the electron mass to zero in the discussion above. Henceforth, we will also set  $m_W = 0$  for simplicity. If the parton subprocess is a  $2 \rightarrow 2$  scattering process, eqs. 2.9 and 2.10 simplify. If  $\delta$  is the squared center-of-mass energy, then  $E_t = \sqrt{\delta}/2$ , which implies that:

$$\cos\theta_e = \pm \sqrt{1 - \frac{4p_T^2}{\delta}} \quad (2.13)$$

$$\cosh(y - y_W) = \frac{\sqrt{\delta}}{2p_T} \quad (2.14)$$

When the  $W$  is on mass shell,  $\delta = m_W^2$ . Then eq. 2.14 can be shown to be identical to eq. 2.7 (with  $m_W = 0$  assumed). We see that the sign ambiguity in eq. 2.13 is a direct consequence of the two-fold ambiguity in determining  $y_W$  (see discussion below eq. 2.7).

Let us contrast the production of a new heavy  $W_L$  and  $W_R$ . Computing the elementary cross section for  $d\bar{d} \rightarrow W_{L,R}^- \rightarrow e^- N$ , we find:

$$\frac{d\sigma}{dE_t d\cos\theta_{ed}} = \frac{\pi\alpha^2 \sqrt{\delta} (1 + \cos\theta_{ed})^2 B_i}{48 \sin^4\theta_W [(m_W^2 - \delta)^2 + \Gamma_W^2 m_W^2]} \delta \left(1 - \frac{2E_t}{\sqrt{\delta}}\right) \quad (2.15)$$

where  $\theta_{ed}$  is the angle between the electron and the  $d$ -quark and  $B_i = \Gamma(W \rightarrow eN)/\Gamma_W$ . The factor of  $(1 + \cos\theta_{ed})^2$  in eq. (2.15)

can be understood using simple helicity arguments as shown in Fig. 1. The  $W_L^-$  couples to a left-handed  $d$ -quark and electron and right-handed  $\bar{u}$ -quark and  $\bar{e}$ . Angular momentum conservation favors  $\theta_{ed}$  near  $0^\circ$  and disfavors  $\theta_{ed}$  near  $180^\circ$ . Similar arguments can be used for the  $W_R^-$  couplings resulting in the same angular distribution. Thus,  $W_L$  and  $W_R$  production cannot be distinguished by only studying the distribution of electrons resulting from  $W \rightarrow eN$  decay. If a gauge boson existed which had a  $V - A$  coupling to  $\bar{d}d$  and a  $V + A$  coupling to  $e^-\bar{N}$  (or vice versa), then one would find a  $(1 - \cos\theta_{ed})^2$  distribution. (The helicity argument analogous to Fig. 1 is straightforward.) This situation could easily be distinguished experimentally from the  $W_L$  or  $W_R$  case; although theoretically, there is no motivation for such bosons.

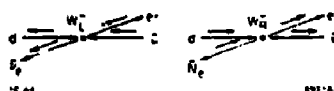


Fig. 1. Schematic view of the process  $\bar{d}d \rightarrow W_{L,R}^- \rightarrow e^- N$ . The arrows above the fermion lines denote helicity. Note that the  $\bar{d}d$  is always right-handed, whereas the  $N$  is always left-handed. Angular momentum conservation implies that the configurations shown above are the ones favored. Hence, the electron angular distribution is the same for both  $W_L$  and  $W_R$  decay.

The electron distributions in the laboratory are obtained by inserting eq. 2.15 into eq. 2.8 (using eqs. 2.9 - 2.12) and performing the integration. It is standard practice to replace the  $W$ -boson propagator with  $\delta\delta(m_W^2 - \delta)/(\Gamma_W m_W)$  in the narrow resonance approximation. However, by doing this one can miss interesting and possibly important effects on the tails of distributions due to virtual  $W$  exchange.

### B. Discovery Limits of New $W$ /Z

The basic signatures of new  $W$ 's and  $Z$ 's are  $W^- \rightarrow e^- N$  and  $Z^0 \rightarrow e^+ e^-$  (or the same reactions with  $e$  replaced by  $\mu$ ). These processes are remarkably background free. This fact has been already evident at the CERN Collider where the  $W(83)$  and  $Z(94)$  were discovered with only a handful of events.<sup>4</sup>

Consider first  $W^- \rightarrow e^- N$ . The discovery of the  $W(83)$  was made by isolating events with the following features:

- the electron was isolated;
- the electron had substantial  $p_T$  (the  $p_T$ -distribution showed the expected peaking at  $p_T \sim m_W/2$ );
- the event tended to be quiet with no appreciable hadronic activity at large  $p_T$ ;
- the event has a large missing transverse momentum due to the undetected neutrino.

In discovering a new heavy charged  $W$ , features (a) and (b) will persist. Features (c) and (d) will depend on the properties of the neutral lepton  $N$ . Ideally, properties (a) and (b) are sufficient to identify a new  $W$ . However, one must keep in mind that electron identification is not 100% efficient. Furthermore, an important property of the  $W(83)$  identification by the UA1 detector was the ability to match momentum and energy of a hypothetical electron track.<sup>38</sup> At the SSC, for extremely energetic electrons, the momentum measurement becomes increasingly difficult (see Section 3). Nevertheless, we believe that

isolated large  $p_T$  leptons are sufficiently rare that such problems can be overcome.

In the case of  $Z^0 \rightarrow e^+e^-, \mu^+\mu^-$ , the situation is easier to analyse. Here, one looks for events with: (a) two isolated electrons (or muons); (b) no appreciable hadronic activity at large  $p_T$ ; and (c) little missing transverse momentum. Energy measurements of the lepton tracks alone allow the invariant mass of the parent  $Z^0$  to be reconstructed. Again, as evidenced by the discovery of the  $Z^0$  (94) at the CERN Collider, the signature of a new  $Z^0$  is extremely clean and devoid of background.

The conclusion we draw from the above discussion is that a new  $W$  and  $Z$  can be discovered on the basis of a small number of events which we shall choose arbitrarily to be ten events per year. Based on this criterion, it is easy to use eq. 2.1 to obtain the "discovery limits" of new  $W$ 's and  $Z$ 's at the SSC, i.e. the maximum mass of such bosons which would result in ten leptonic (either  $e$  or  $\mu$ ) events per year. This analysis was performed by EHLQ and by LRR in the approximation that the produced gauge boson was on-shell (narrow width approximation). The results, using the criterion for discovery described above, are summarized in Table 3. Further discussion on discovery limits at the SSC will be given in Section 4A.

Table 3

	$p_T$	$\bar{p}_T$
$W_L^+, W_R^+$	8.6	6.5
$W_L^-, W_R^-$	7.3	6.5
$Z^0$	6.5	5.0
$Z_L^0$	5.6	3.8

Table 3: The discovery limits of new heavy gauge bosons at the SSC. We assume that  $\sqrt{s} = 40$  TeV and  $\mathcal{L} = 10^{33} \text{ cm}^{-2} \text{ sec}^{-1}$  for  $pp$  or  $\mathcal{L} = 10^{32} \text{ cm}^{-2} \text{ sec}^{-1}$  for  $\bar{p}p$ . The discovery limits are obtained by requiring that 10 leptonic events per year ( $10^7 \text{ sec}$ ) be observed. The masses above are given in units of TeV. The above numbers were obtained from ref. 1, except for the  $Z^0$  entries which were obtained from ref. 6. The properties of  $Z^0$  and  $Z_L^0$  are given in Table 2.

One further feature of new  $W$  and  $Z$  production is worth noting here. Let us assume that the new gauge boson produced is rather heavy (say, of order 1 TeV). Then, a large fraction of the cross section is produced in the central region. This is illustrated in Fig. 2 (taken from LRR) where we plot the rapidity distribution of a new  $Z^0$  with a mass of 1 TeV. We remind the reader that  $|y| = 3$  corresponds to an angle  $5^\circ$  with respect to the beam axis.

### C. Asymmetries

We have argued in the previous section that if new  $W$ 's and  $Z$ 's exist with masses less than those listed in Table 3, then it should be possible to verify their existence at the SSC. In order to understand the theoretical implications of new gauge bosons, it is necessary to explore the properties of such bosons - specifically, their couplings to quarks and leptons. This is by no means a trivial task. Whereas ten events per year is sufficient to identify the existence of a new gauge boson, one will need hundreds (or more) events to determine aspects of its couplings. Furthermore, observation of electrons from the decays  $W \rightarrow eN$  and  $Z \rightarrow e^+e^-$  alone will leave many ambiguities as to some of the gauge boson properties. As an example, as we saw at the end of

Section 2A, one cannot distinguish  $W_L$  from  $W_R$  on the basis of the electron distributions. Nevertheless, partial information can be obtained by studying various asymmetries which we define below. Here we follow closely the papers of LRR.

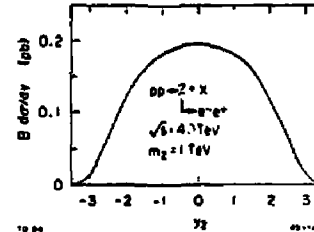


Fig. 2 The rapidity ( $y_Z$ ) distribution for a new  $Z$  of mass 1 TeV in  $pp$  scattering at  $\sqrt{s} = 40$  TeV.  $B$  is the branching ratio into  $\mu^+\mu^-$ . The couplings of the  $Z^0$  to fermions correspond to those of  $Z_L$  listed in Table 2. This graph was taken from LRR.

**1. Forward - Backward Asymmetries.** Consider the process  $A + B \rightarrow W_{L,R}^- + X, W_{L,R}^- \rightarrow e^-N$ . Let us assume that the rapidity of the  $W^-$  can be determined. Then, the kinematics of the parton subprocess  $Qd \rightarrow W^-$  are entirely fixed. Given  $y_W$ , we can obtain  $x_1$  and  $x_2$  by eq. 2.2 and the parton center-of-mass scattering angle  $\hat{\theta}_e$  by eq. 2.10. We may choose  $y_W$  and  $\cos \hat{\theta}_e$  to be the independent variables. Then, using eqs. 2.6 and 2.15,

$$\frac{d\sigma}{dy_W d\cos \hat{\theta}_e} = N \left[ d^A(x_1) d^B(x_2) (1 + \cos \hat{\theta}_e)^2 + d^A(x_1) d^B(x_2) (1 - \cos \hat{\theta}_e)^2 \right] \quad (2.16)$$

where  $N$  is an appropriate normalising factor. Note that we have identified  $\hat{\theta}_e = \hat{\theta}_{et}$  and  $\hat{\theta}_e = \pi - \hat{\theta}_{et}$  in the two terms respectively. For fixed  $y_W$ , define the forward-backward asymmetry by

$$AFB = \frac{F - B}{F + B} \quad (2.17)$$

where

$$F \pm B = \left[ \int_0^{\frac{\pi}{2}} \pm \int_{-\frac{\pi}{2}}^0 \right] d\cos \hat{\theta}_e \frac{d\sigma}{dy_W d\cos \hat{\theta}_e} \quad (2.18)$$

Then, for example, for  $A + B \rightarrow W_{L,R}^- + X, W_{L,R}^- \rightarrow e^-N$

$$AFB(y_W) = \frac{3}{4} \frac{d^A(x_1) d^B(x_2) - d^A(x_1) d^B(x_2)}{d^A(x_1) d^B(x_2) + d^A(x_1) d^B(x_2)} \quad (2.19)$$

We remind the reader that  $x_1, x_2 = (m_W/\sqrt{s})^{1/2} y_W$ .

First consider  $pp$  scattering. Taking  $A$  to be the proton, we see that in a regime where valence quarks dominate  $d^A d^B \gg d^A d^B$  implying  $AFB \approx \frac{3}{4}$ . In fact, we can integrate over  $y_W$  as well without diluting the signal; the advantage being that less data is required to see an effect. In  $\bar{p}p$  scattering, there is also an asymmetry. This first comes as a surprise since one apparently can argue that there is no inherent direction defined

in  $p\bar{p}$  scattering. However, by measuring  $y_W$ , one determines the direction of the  $W^-$  in the laboratory on an event-by-event basis. In addition, eq. 2.15 (or Fig. 1) implies that the electron tends to follow the direction of the  $d$ -quark. Thus, at a fixed non-zero  $y_W$ , one can determine on a statistical basis which proton the  $d$ -quark came from. Thus a non-zero asymmetry exists for  $y_W \neq 0$  as shown in eq. 2.19. Of course at  $y_W = 0$ , there is no preferred direction remaining and hence no asymmetry.

The one loophole in the above arguments is the assumption that  $y_W$  is known. As shown below eq. 2.7, there is usually a two-fold ambiguity in the determination of  $y_W$ . What is more troublesome is that the ambiguity in  $y_W$  leads to a sign ambiguity in  $\cos \theta$ , as exhibited in eq. 2.13. This problem appears to ruin the computation of the asymmetry. However, as argued previously, one can often rule out one of the two solutions for  $y_W$  on the basis of the event kinematics. Otherwise, one must define an unambiguous variable on an event-by-event basis (such as  $\hat{y}$  — see discussion below eq. 2.7). At present, further analysis is required to see whether  $A_{FB}$  is a useful quantity in charged  $W$  production (if the neutral lepton is not detected). Of course, if the  $N$  decays and can be reconstructed, then one will be able to measure directly  $y_W$  unambiguously, and the above problems disappear.

The asymmetry  $A_{FB}$  in  $Z^0$  production can be derived in a similar manner. For example, for  $Z^0 \rightarrow e^+e^-$  one computes  $A_{FB}$  for one of the leptons. In this case, the rapidity of the  $Z^0$  is directly measured in the laboratory by measuring the four-momentum of the  $e^+e^-$  system. Explicit formulas have been computed by LRR, and many graphs of  $A_{FB}(y)$  for various gauge bosons can be found there.

From the discussion above, it is clear that the measurement of the electric charge of the lepton is of extreme importance to the program of measuring asymmetries. For example, it is easy to show that:

$$A_{FB}(p\bar{p} \rightarrow W^+) + A_{FB}(p\bar{p} \rightarrow W^-) = 0 \quad (2.20)$$

so that without a sign measurement,  $A_{FB}$  would vanish in  $p\bar{p}$  scattering. In  $p\bar{p}$  scattering, there would be an observable asymmetry even if electric charge was not measured. Such an asymmetry would test the relative strength of the  $W$  or  $Z$  to  $u$  and  $d$  quarks, but would be insensitive to the helicity structure of the gauge boson couplings.

2. Global Asymmetries. For completeness, we mention some global asymmetries considered by LRR. These have the virtue that fewer events are required in order to see an effect. The average front-back asymmetry ( $A_F$ ) is obtained by integrating the numerator and denominator of eq. 2.17 over  $y_W$ . It is non-zero in  $p\bar{p}$  scattering but is exactly zero for  $p\bar{p}$  scattering (as there is no preferred direction). In  $p\bar{p}$  scattering, a useful asymmetry is

$$A_E \equiv \frac{\langle E_{t+} \rangle - \langle E_{t-} \rangle}{\langle E_{t+} \rangle + \langle E_{t-} \rangle} \quad (2.21)$$

where  $\langle E_t \rangle$  is the average lepton energy measured in the laboratory. Graphs of  $\langle E_t \rangle$  for various new gauge bosons have been computed by LRR. Note that  $CP$  invariance implies that in  $p\bar{p}$  scattering,  $A_E = 0$ .

#### D. Polarized Beams

In the previous section, we presented the study of asymmetries as one method for gaining information on the nature of the couplings of new  $W$ 's and  $Z$ 's to fermions. However, this technique can only provide partial information; for example, it cannot distinguish  $W_L$  and  $W_R$ . One method for obtaining a more complete description of the underlying couplings is to study new  $W$  and  $Z$  production from polarized beams.

The literature contains a number of studies on the power of polarized beams<sup>38</sup> in analysing the properties of the  $W(83)$  and  $Z(94)$ .<sup>40</sup> These techniques can be generalised in a straightforward manner to encompass new  $W$  and  $Z$  production at the SSC. However, such work has not yet been performed. It was a deliberate decision of the New  $W/Z$  Physics Subgroup to refrain from considering in detail implications of polarized beams to new  $W$  and  $Z$  physics. It is clear that polarized beams provide a very useful tool for investigating details of new  $W$  and  $Z$  couplings to fermions. We believe that it is more appropriate to perform a careful and complete analysis on the polarization effects for new  $W$  and  $Z$  production rather than to take the cursory approach which would have been necessary at Snowmass. Furthermore, it is clear that polarization phenomena would be at best a feature of second generation experiments at the SSC. At present, we are aware of no realistic studies as to the feasibility of polarized beams at the SSC. Hence, we felt that a theoretical analysis of polarization phenomena could be postponed in favor of the topics discussed in Sections 3 and 4.

Before leaving this topic, a few comments are appropriate. In the study of hard scattering with polarized beams, one needs to know the spin-dependent structure functions.<sup>41,42</sup> Here our experimental knowledge is not as precise (as compared to the determination of the unpolarized structure functions) since the data on polarized lepton production is limited.<sup>39</sup> Nevertheless, there have been attempts to provide a reasonable set of spin-dependent structure functions. (A recent analysis which obtains spin-dependent structure functions by direct resolution of the spin-dependent Altarelli-Parisi equations has been given by Chiappetta and Soffer.<sup>42</sup>)

It is expected that the helicity of a polarized proton is carried primarily by the valence quarks. Let us define  $u_+(z)(u_-(z))$  to be the probability of finding a positive (negative) helicity valence  $u$ -quark inside a positive helicity proton. The simplest model would be to say that  $u_+(z) = 5/6 u^0(z)$ ,  $u_-(z) = 1/6 u^0(z)$ ,  $d_+(z) = 1/3 d^0(z)$ , and  $d_-(z) = 2/3 d^0(z)$  on the basis of the spin composition of the quark content of the  $SU(6)$  wavefunction of a positive helicity proton. Carlitz and Kaur<sup>41</sup> presented a more sophisticated model based on the idea that valence quarks carry the proton helicity only at large values of  $z$ . They proposed:

$$u_+(z) = \frac{1}{2} u^0(z)[1 + f(z)] - \frac{1}{3} d^0(z)f(z) \quad (2.22a)$$

$$d_+(z) = \frac{1}{2} d^0(z)[1 - \frac{1}{3} f(z)] \quad (2.22b)$$

$$u_-(z) = u^0(z) - u_+(z) \quad (2.22c)$$

$$d_-(z) = d^0(z) - d_+(z) \quad (2.22d)$$

$$f(z) = [1 + H_0 z^{-1/2} (1 - z)^2]^{-1} \quad (2.22e)$$

and  $H_0 = 0.032$  has been adjusted so that the Bjorken sum rule is satisfied. Note that as  $z \rightarrow 0$ ,  $u_+(z) = u_-(z) = 1/2 u^0(z)$  and  $d_+(z) = d_-(z) = 1/2 d^0(z)$ . As  $z \rightarrow 1$ , we approach the

$SU(6)$  limit previously mentioned, if in addition we impose the  $SU(6)$  inspired relation,  $\alpha' = 1/2 \alpha^0$ . One convenient feature of eqn. 2.22 is that the EHLQ structure functions may be inserted to obtain spin-dependent structure functions which are sensible for SSC physics.

The above discussion suggests that polarised beams will be of little interest for processes which result from the scattering of small- $x$  and/or non-valence partons. However, this is certainly not the case in the production of (sufficiently heavy) new  $W$ 's and  $Z$ 's. Let  $\sigma_{++}$  denote the total cross section for  $p_+ p_+ \rightarrow W$  where the protons are polarised as indicated. In  $p\bar{p}$  scattering, gauge bosons are produced by the scattering of two valence quarks so polarization effects (e.g.  $\sigma_{--} > \sigma_{++}$  for  $W_L$ ) can be significant. Furthermore, in  $p\bar{p}$  scattering,  $W^\pm$  production cross sections are equal, so that one need not measure the sign of the outgoing lepton to see such effects. In  $p\bar{p}$  scattering, one valence quark is involved in the scattering and effects due to polarization are still visible. Here the situation is more complicated and sign information can be important. For example, we find that for  $W_L^+$ ,  $\sigma_{--} > \sigma_{++}$  but the reverse is true for  $W_L^-$ . (For  $W_R$ , reverse the sign of all inequalities above.) We emphasise that effects can be large with  $\sigma_{--}/\sigma_{++}$  of order 2% for 100% polarised beams. Careful computations are required in the case of partial polarization. Other interesting observables have been studied in the literature.<sup>38,40</sup> One needs to develop this further, and determine which observables are best in order to untangle unknown new  $W$  and  $Z$  couplings.

### 3. Experimental Issues Related to the Physics of New $W$ 's and $Z$ 's at the SSC

[This section was written by S. Aronson and B. G. Pope]

#### A. Prelude

New  $W$  and  $Z$  gauge bosons were taken to be detectable via two generic decays:

$$W^\pm, Z^0 \rightarrow \text{jets}, \quad (3.1)$$

and

$$W^\pm, Z^0 \rightarrow \text{leptons}, \quad (3.2)$$

e.g.

$$W_R^\pm \rightarrow \ell^\pm N; Z^0 \rightarrow \ell^+ \ell^- \quad (3.3)$$

where  $N$  is a (heavy) neutral lepton.

The experience at  $SppS$  with jet decays of heavy states has so far been less than encouraging for this line of attack. Consequently we left this topic for harder work and focussed on the leptonic decays. In this case, high- $p_T$  leptons (plus missing  $p_T$ ) have been spectacular successful tools at  $SppS$ .

In the present case, however, where one expects to look for heavy gauge bosons at masses  $\lesssim 10$  TeV, we considered the problem of identifying and measuring  $\mu$ 's and  $e$ 's with  $p_T$  in excess of 1 TeV. In the next section we explore the consequence of using conventional techniques for studying these very stiff leptons.

#### B. Detecting and Measuring Leptons

1. **Electrons.** Electron identification will rely primarily on fine-grained calorimetry; magnetic analysis will enhance the identification ( $E$  vs.  $p$ ) and of course will provide the desired sign determination. Design studies for the  $D0$  detector<sup>41</sup> and similar

devices have shown that the calorimeter should have good longitudinal segmentation (for  $e/\text{hadron}$  discrimination) and good transverse segmentation (for rejection of  $\gamma$ -hadron overlap). As an example,  $D0$  has about 50,000 channels of calorimetry surrounding a very compact (0.7 m radius, no magnet) inner tracking system. A similarly fine-grained calorimeter surrounding an adequate magnetic tracking system (see below) might easily have an order of magnitude more channels.

Other devices, such as transition radiation or synchrotron radiation detectors might also enhance the electron identification; these could be interspersed among the tracking chambers.

As for the magnetic tracking system, we relied on a PSSC<sup>42</sup> study to guide our estimates. Figure 3, from the PSSC summary report indicates the field integral needed in conjunction with a large but conventional drift chamber. Assuming that a reliable sign determination is equivalent to a 30% momentum measurement, a 1.5 T, 3.5 m radius magnet is seen to be required to reach the several - TeV range of interest. While a more sophisticated chamber might improve on the assumed 200  $\mu\text{m}$  resolution, it should be noted that using  $E$  vs.  $p$  as an electron identification tool probably requires a better than 30% momentum measurement.

2. **Muons.** The conventional approach features a hadron absorber followed by magnetic analysis. Tracking before the absorber is also very important. At least, this front tracking can locate the event vertex which is very helpful in muon triggering if the source is of finite extent. At best the  $\mu$ -candidate can be seen in the front tracker and its momentum matched to that in the rear. Muon backgrounds result from hadron punch through and from  $\pi$  or  $K$  decay. The former is addressed with a very thick absorber ( $D0$  has  $\geq 10$  everywhere) and external magnetic analysis. The latter can be handled by having a very compact space ahead of the absorber (in direct conflict with the good tracking needed for electrons!) and/or by seeing the decay kink (which would probably require a precision vertex chamber).

#### C. How Well Can One Measure the Width of a New $Z^0$ ?

The following analysis is presented courtesy of Tom O'Halloran. Suppose we measure the mass of the new  $Z^0$  from its  $e^+ e^-$  decay. If we denote by  $\theta$  the opening angle of the  $e^+ e^-$  pair, then we have (approximately, for small  $\theta$ )  $M_Z^2 \approx E_1 E_2 \theta^2$ . Thus, only electron energies are required and these can be measured quite accurately at high energies. The expected measurement error in the mass is then:

$$\frac{\Delta M_Z}{M_Z} \approx \frac{1}{2} \left[ \left( \frac{\Delta E_1}{E_1} \right)^2 + \left( \frac{\Delta E_2}{E_2} \right)^2 + 4 \left( \frac{\Delta \theta}{\theta} \right)^2 \right]^{1/2} \quad (3.4)$$

The error in the energy measurement in the calorimeter takes the form:

$$\frac{\Delta E}{E} = a + \frac{b}{\sqrt{E}} \quad (3.5)$$

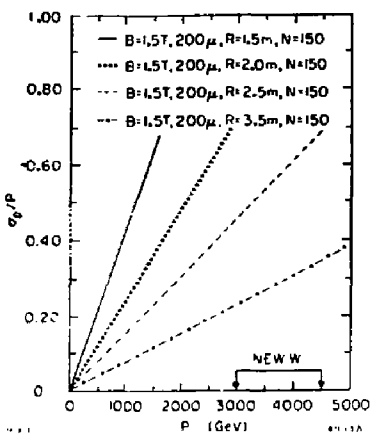


Fig. 3. The momentum resolution for various magnetic spectrometer parameters.  $R$  is the chamber radius, the magnetic field is taken to be  $1.5\text{ T}$ , the spacial resolution is  $200\text{ }\mu\text{s}$  and 150 samples are assumed. The arrows represent the range of maximum lepton momenta possible at  $\sqrt{s} = 40\text{ TeV}$  from the decay of a new  $W$ . This figure is taken from Ref. 44.

For sufficiently high energy electrons, the  $b/\sqrt{E}$  term becomes negligible and the constant term dominates. With present techniques, the best we can imagine is to have  $a \approx 0.01$ . Now,  $\Delta\theta/\theta$  depends on the geometry of the detector and is hard to estimate. Let us assume that  $(\Delta E_1/E_1)^2 + (\Delta E_2/E_2)^2 \approx 4(\Delta\theta/\theta)^2$ , i.e. the detector is designed to match the energy and angular errors (there is not much sense in doing better). We conclude that:

$$\frac{\Delta M_2}{M_2} \approx 0.01 \quad (3.6)$$

This is to be compared with the expected  $Z^0$  width; typically  $\Gamma_Z/M_2 \sim 0.03$ . This indicates that with a sufficiently large data sample, it should be possible to measure the new  $Z^0$  mass with a resolution smaller than its natural width at the SSC.

#### D. Schematic Detector for Both $e$ and $\mu$

Figure 4 shows a combined-function lepton detector; it is a deep, fine grained calorimeter/absorber with magnetic tracking fore and aft. Although it is shown as a detector "arm" of modest solid angle, the reader may imagine a more hermetic device built along the same lines. The gargantuan scope of the resulting detector raises some immediate questions:

**1. Does one need this capability over  $4\pi$ ?** The answer to this question may have more to do with the rest of the event than with the  $e$ 's and  $\mu$ 's. For example, in the decay  $W_N^{\pm} \rightarrow \ell^{\pm} N$ , the  $N$  may behave in a neutrino-like way (i.e. appear as missing  $p_T$  in a hermetic detector) or it may decay to visible products at the primary or a secondary vertex. More theoretical study of  $N$  decays may help establish the effect of unstable  $N$ 's on the signatures, but it may be that microvertex detectors are more important than  $4\pi$  coverage.

If the answer to question 1 is yes, a "super L3" ( $20\text{ m} \times 20\text{ m} \times 20\text{ m}$ ) is the result of this conventional attack on the problem.

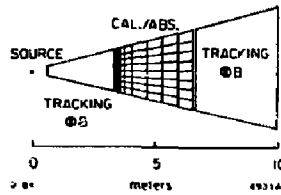


Fig. 4 A schematic SSC detector for detecting electrons and muons.

**2. Does one need full  $e$  and  $\mu$  capability?** If, for example, one were to drop the requirement of sign determination on the electrons, one might scrape by with a standard L3, instead of the Super L3 mentioned above. Other such modest fall-back positions might suggest themselves as other requirements are relaxed.

**3. Can one measure the decay asymmetry?** Gollin<sup>45</sup> has recently considered the possibility of measuring front-back asymmetries for a new  $Z^0$  decaying into  $\mu^+\mu^-$ . He performed a Monte Carlo simulation of a 2500 ton muon spectrometer. His conclusions are that a reasonable measurement of  $A_{FB}$  can be made for a new  $Z^0$  of mass  $1\text{ TeV}$  in one year of data taking at the SSC.

**4. Can one distinguish  $W_L$  from  $W_R$ ?** The energy and angular distributions expected from the electron decay of a  $W_R$  are the same as that expected from a  $W_L$ . However, there have been suggestions that the two-step process

$$W \rightarrow \tau N, \tau \rightarrow e \nu \bar{\nu} \quad (3.7)$$

might distinguish  $W_L$  from  $W_R$  in the electron energy distribution. In order to identify  $\tau$ 's a microvertex detector would be essential, but even then the measurement would be extremely difficult. Other decay modes of the  $\tau$  (e.g.  $\tau \rightarrow \pi$  or  $\rho + \nu$ ) may provide a better means of identifying the  $\tau$ . Further work is required to determine how high an efficiency for  $\tau$ -detection can be attained at the SSC.

**5. What other physics can be done with this detector?** Although motivated by searches for heavy gauge bosons, the detectors imagined here (surely all in the  $\$100\text{ M}$  class) are likely to have other physics potentialities. More communication with the other physics groups would have helped answer this question. It is clear that any real device (especially of this scope) would have to attack a very broad range of questions in the multi-TeV range to justify itself.

#### 4. The Physics of New $W$ 's and $Z$ 's at the SSC - Theoretical Issues

In this section, we summarise the theoretical work of the New  $W/Z$  Physics Subgroup.

##### A. Discovery Limits Revisited

The potential discovery limits for new  $W$ 's and  $Z$ 's were considered both for the case of  $pp$  collisions (at  $\sqrt{s} = 40\text{ TeV}$ ) and for two proposed versions of the  $ep$  option at the SSC. We discuss the latter case first.

Two options for  $ep$  collisions at the SSC were studied.<sup>46</sup> The first was a low energy option -  $30\text{ GeV}$  electrons colliding with

20 TeV protons. Luminosities greater than  $10^{32} \text{ cm}^{-2} \text{ sec}^{-1}$  are conceivable and electron polarization up to about 80% seems plausible. The  $ep$  option subgroup determined that such an  $ep$  collider at the SSC was feasible. The second option considered was 140 GeV electrons colliding with 20 TeV protons. The  $ep$  option subgroup was unable to come up with a feasible design for this higher energy facility. The theoretical issues relevant for  $ep$  colliders (including new  $W/Z$  physics) were considered in detail by Gunion.<sup>47</sup> Further analysis has also been provided by Gunion and Kaiser.<sup>48</sup> Here, we briefly summarize their conclusions.

In  $ep$  collisions, one can hope to detect a new heavy  $W_R$  boson by observing evidence of its virtual exchange as shown in Fig. 5. There are three basic methods to see evidence of a new  $W_R$ : (a) detect a rate enhancement beyond that expected by the Standard Model process  $e^-p \rightarrow \nu + X$  via  $W(83)$  exchange; (b) detect evidence of a right-handed current by studying the rate for the charged current process as a function of electron polarization; and (c) detect the decay of a new neutral heavy lepton  $N$ . The advantage of the low energy  $ep$  option is that substantial electron polarization may be possible which can greatly enhance the signal over the large background coming from virtual  $W(83)$  exchange.

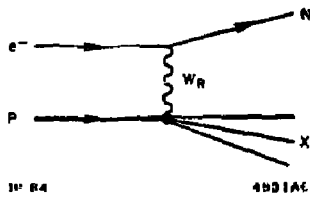


Fig. 5. Feynman diagram for electro-production of a neutral heavy lepton via the exchange of a  $W_R$  gauge boson.

In general, the rate for the charged current process via  $W(83)$  exchange will dominate the exchange of some new heavy  $W$  due to propagator effects.<sup>49</sup> This suggests that it will be necessary to make a strong  $Q^2$  cut (e.g. only accept events with  $Q^2 \gtrsim 1/2 M_{W_R}^2$ ) in order to reduce the large background.<sup>48</sup> An example of the effects of the  $Q^2$  cuts is provided in Table 4, (calculations courtesy of J. F. Gunion and B. Kaiser). Note in particular that although the signal-to-noise is far better for the higher energy electron beam, one obtains substantial improvement at the lower energy machine if a polarized electron beam is used, assuming that the new heavy  $W$  is right-handed. The conclusion here is that for both  $ep$  options considered, a new heavy  $W_R$  with mass 1.6 TeV is near the detection limit. This is substantially less than the discovery limits of new  $W$ 's and  $Z$ 's at hadron-hadron colliders with  $\sqrt{s} \geq 10$  TeV. Therefore, it seems clear that hadron-hadron colliders are the most suitable to study new  $W/Z$  physics.

Table 4  
(a)  $M_{W_R} = 1.6 \text{ TeV}$  Number of events

$E_e$	Polarization	$Q^2$	$ep \rightarrow eX$	$ep \rightarrow \nu X$	$ep \rightarrow NX$
30	none	0.50	200	250	10
30	80% $e_R^+$	0.50		50	20
140	none	2.56	20	60	15

(b)  $M_{W_R} = 1.0 \text{ TeV}$  Number of events

$E_e$	Polarisation	$Q^2$	$ep \rightarrow eX$	$ep \rightarrow \nu X$	$ep \rightarrow NX$
30	none	0.50	200	300	40
140	none	0.64	1000	2300	550

Table 4: Calculation of the number of charged and neutral current events at an  $e^-p$  collider assuming an integrated luminosity of  $10^{10} \text{ cm}^{-2}$ . The energy of the electron beam is  $E_e$  (in GeV units) and the energy of the proton beam is 20 TeV. The processes  $ep \rightarrow eX$  and  $ep \rightarrow \nu X$  occur via the Standard Model mechanism, whereas  $ep \rightarrow NX$  involves the exchange of a  $W_R$  boson (two possible masses are considered). We apply a  $Q^2$  cut; keeping only those events with  $Q^2 > Q_0^2$  ( $Q_0^2$  is given in units of  $\text{TeV}^2$ ). The number of events passing the cut are listed above. In one case above, we exhibit the effects of having an 80% right-handed polarized electron beam on the charged current processes.

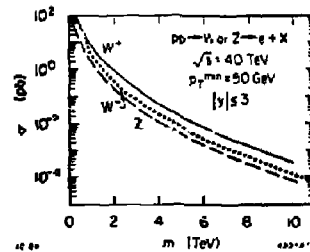


Fig. 6. Integrated single lepton spectrum resulting from new gauge bosons  $W^2$  and  $Z^0$  plotted vs. the new gauge boson mass. The  $W^2$  is either  $W_L^2$  or  $W_R^2$ . The  $Z^0$  couplings to fermions are identical to those of the  $Z^0$ (pd) (see Table 2). We demand that the single lepton satisfy  $p_T \geq 50 \text{ GeV}$  and  $|y| \leq 3$ .

The discovery limits of new  $W$ 's and  $Z$ 's at the SSC for both  $pp$  and  $p\bar{p}$  collisions have been given by EHLQ and LRR. A number of refinements to these calculations were made by Gunion; his results are presented in a separate contribution.<sup>49</sup> Only new  $W$  production will be discussed here, the signal consists of an isolated electron arising from  $W \rightarrow eN$ . The new features are as follows. Previous calculations made use of the narrow width approximation for the  $W$ , i.e. the produced  $W$  was on-shell. It is a simple matter to include the effects of the full  $W$  propagator. This has an effect of substantially broadening the tail of the  $p_T$ -distribution of the observed electron beyond the Jacobian peak  $p_T \gtrsim M_W/2$ . In addition, we make cuts on the outgoing electron rapidity and  $p_T$  by taking only events with  $|y| \leq 3$  and

$p_T \geq 50$  GeV. The resulting total  $W$  and  $Z$  cross sections (times leptonic branching ratio) are shown in Fig. 6. The dominant background consists of electrons arising from virtual  $W$  (83) production as shown in Figs. 7 and 8. This confirms our previous claim that, the production of a new  $W$  is nearly background free and should be discoverable on the basis of a handful of events. The conclusion of the above analysis is that the discovery limits obtained by LRR (see Table 3) should be quite reasonable.

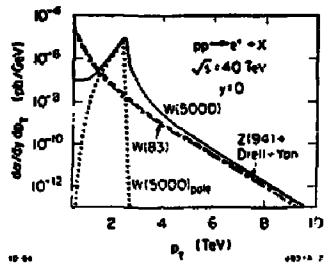


Fig. 7. Single lepton  $p_T$ -spectrum at  $y = 0$  resulting from the leptonic decay of a new  $W_L^+$  or  $W_R^+$  with mass of 5 TeV. The complete result (allowing for virtual as well as real  $W$ 's) and the pole approximation are both depicted. Also shown are single lepton backgrounds resulting from virtual  $W^+(83)$ , virtual  $Z^0(94)$  and Drell-Yan production.

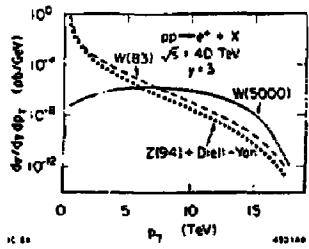


Fig. 8. Single lepton  $p_T$ -spectra at  $y = 3$ . See caption to Fig. 7. The pole approximation is not shown as it is nearly identical to the complete result, in this case.

## B. Asymmetries Revisited

Suppose a new  $W$  or  $Z$  is discovered at the SSC. One will then attempt to learn details of its couplings to fermions. Clearly, if the mass of the new vector boson is near the discovery limits of Table 3, then there will not be sufficient statistics to determine the vector boson couplings. Thus, it is useful to estimate the maximum value of the mass of a new vector boson for which detailed information regarding its properties can be extracted.

As an example of the kind of analysis we envisioned, Deshpande, et al.<sup>30</sup> considered the front-back ( $y$  dependent) asymmetry introduced by LRR which we have discussed in Section 3C. We focussed on the production of a new neutral  $Z^0$  boson,

where its rapidity can be directly determined by measuring the  $Z^0 \rightarrow e^+ e^-$  decay. In this case, the formulae for the front-back asymmetry can be conveniently written as follows. First define three functions  $f_i(y)$ ,  $i = 1, 2, 3$ :

$$f_1(y) = \frac{u^A(z_1)u^B(z_2) - u^A(z_1)v^B(z_2)}{u^A(z_1)u^B(z_2) + u^A(z_1)v^B(z_2)} \quad (4.1)$$

$$f_2(y) = \frac{d^A(z_1)d^B(z_2) - d^A(z_1)d^B(z_2)}{u^A(z_1)u^B(z_2) + u^A(z_1)v^B(z_2)} \quad (4.2)$$

$$f_3(y) = \frac{d^A(z_1)d^B(z_2) + d^A(z_1)v^B(z_2)}{u^A(z_1)u^B(z_2) + u^A(z_1)v^B(z_2)} \quad (4.3)$$

where

$$z_1 = M_Z e^y \quad (4.4a)$$

$$z_2 = M_Z e^{-y} \quad (4.4b)$$

and  $q^A(x)$  is the probability of finding quark  $q$  in hadron  $A$  at momentum fraction  $x$  and at an energy scale  $Q = M_Z$ . These functions can be determined using EHLQ structure functions; we depict the functions for  $M_Z = 0.5$  and 1.5 TeV in Figs. 9 and 10. The front-back asymmetry,  $A_{FB}(y)$  is then determined in terms of the functions  $f_i$  ( $i = 1, 2, 3$ ) and parameters which depend on the couplings of the  $Z$  to fermions:

$$A_{FB}(y) = \frac{C[\alpha f_1(y) + \beta \gamma f_2(y)]}{1 + \gamma f_3(y)} \quad (4.5)$$

where

$$C = \frac{3}{4} (L_c^2 - R_c^2) \quad (4.6a)$$

$$\alpha = L_c^2 - R_c^2 \quad (4.6b)$$

$$\beta = L_c^2 - R_c^2 \quad (4.6c)$$

$$\gamma = \frac{g_{Z2J}^2}{g_{Z1J}^2} \quad (4.6d)$$

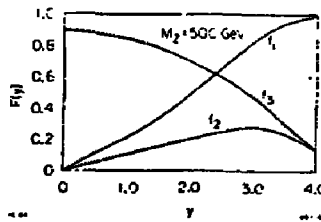


Fig. 9. Graphs of the functions  $f_i(y)$ ,  $i = 1, 2, 3$  (defined by eqs. 4.1 - 4.3) which are relevant to the calculation of asymmetries in  $Z^0 \rightarrow e^+ e^-$  (see eq. 4.5). We take  $M_Z = 500$  GeV.

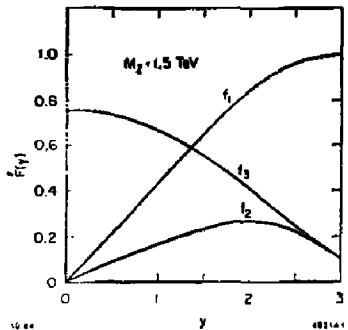


Fig. 10. Graphs of the functions  $f_i(y)$ ,  $i = 1, 2, 3$  for  $M_2 = 1.5$  TeV. See caption to Fig. 9.

The couplings above are normalized,  $L_i^2 + R_i^2 = 1$ , where  $L_i$  is the coupling of  $Z$  to  $f_{iL} \tau^a f_{iL}$  (with a similar definition for  $R_i$ ); and  $\gamma$  measures the relative strength of the  $Zu\bar{u}$  and  $Zd\bar{d}$  squared couplings. Thus, in principle, the quantities  $C\alpha$ ,  $C\beta$ , and  $\gamma$  can be independently measured. We see that this method can only obtain partial information on the  $Z^0 f\bar{f}$  couplings. For example if the  $L$  and  $R$  type coupling are universally interchanged,  $C\alpha$  and  $C\beta$  remain unchanged so that no difference would be seen in the measured value of  $A_{FB}(y)$ .

With a sufficient data sample, it is straightforward to isolate the three parameters  $C\alpha$ ,  $C\beta$  and  $\gamma$  because the functions  $f_i$  ( $i = 1, 2, 3$ ) are sufficiently different as shown in Figs. 9 and 10. Note that although we have obtained Figs. 9 and 10 using EHLQ structure functions, which is an extrapolation from present day data, one can presumably measure the structure functions directly at the SSC thereby obtaining more reliable predictions for the  $f_i$ . The best way to proceed then is to measure the  $y$  distribution of  $Z^0$  production in bins of say, 0.5 units of rapidity. Since  $f_1$  is quite different from  $f_2$  and  $f_3$  at larger rapidities, the parameter  $\gamma$  can be determined by careful measurements in the region  $2 \leq y \leq 3$ . The quantities  $C\alpha$  and  $C\beta$  are then obtained by comparing  $A_{FB}(y)$  at other values of the rapidity. Details of some numerically worked out examples for different mass values of a new heavy  $Z$  which have different couplings to the fermions are presented by Deshpande, et al., in a separate contribution.<sup>50</sup>

Our conclusions are that for masses below 1-2 TeV, it should be possible to determine certain combinations of  $Z^0 f\bar{f}$  couplings ( $C\alpha$ ,  $C\beta$  and  $\gamma$ ; see eq. 4.6) with reasonable accuracy by measuring the  $y$ -dependent front-back asymmetry. The precise upper limit for the  $Z^0$  mass which allows for such a reasonable measurement will depend on the values of the  $Z^0 f\bar{f}$  couplings.

### C. Decay of New $W/Z$ 's Into Tau Leptons

In the last section, we saw that only a limited amount of information on the coupling of new  $W$ 's and  $Z$ 's to fermions can be deduced from the study of asymmetries. A most glaring

example of this is the inability of differentiating  $W_L$  from  $W_R$  by studying unpolarized  $pp \rightarrow W + X$ ,  $W \rightarrow e^- N$  where the signal consists of an isolated electron and the  $N$  is undetected. Further information could be deduced by detecting an explicit decay mode of the  $N$ , although this depends on knowing the mechanism of  $N$  decay (see Section 4E). Here, we shall focus on another method - the possibility of observing  $\tau$ -leptons arising from new  $W$  or  $Z$  decays.<sup>51,52</sup> The key observation here is that the  $\tau$ -decay is self-analyzing. That is, by measuring the spectrum of  $\tau$ -decay products, one obtains information on the emitted  $\tau$  polarization. This is because the  $\tau$  decay mechanism is known, i.e. it decays by emission of a virtual  $W(83)$  ( $W_L$ -type) gauge boson. This in turn can clarify the properties of the new  $W$  and/or  $Z$  which decays into the observed  $\tau$ .

The major decay modes of the  $\tau$  are:  $\tau\nu$ , ( $BR = 22\%$ ),  $\pi\nu$ , ( $BR = 10\%$ ),  $e\nu_e\nu$ , ( $BR = 17\%$ ), and  $\mu\nu_e\nu$ , ( $BR = 18\%$ ).<sup>53</sup> The signal for  $W \rightarrow \tau N$ ,  $\tau \rightarrow \ell\nu$  is similar to that of  $W \rightarrow eN$ , i.e. an isolated lepton  $\ell = e$  or  $\mu$  is observed. However the  $p_T$ -spectrum of the observed lepton arising from  $\tau$  decay (i.e. the indirect lepton) is quite different from the direct lepton. First, the indirect lepton tends to come out at smaller  $p_T$  substantially below the Jacobian peak. Second, the  $p_T$ -distribution of the indirect leptons can distinguish between  $W_L$  and  $W_R$ . But, there are major problems with an attempt to detect  $\tau$ -leptons through its leptonic decay. As shown by Gunion and Haber,<sup>52</sup> the spectrum of indirect leptons (from  $\tau$ -decays) is buried underneath the spectrum of direct leptons for  $p_T \gtrsim 0.2 M_W$  as shown in Fig. 11. For the distributions at  $y = 0$ , this occurs as a result of a prominent Jacobian peak in the direct lepton spectrum. Such a feature persists for non-zero  $y$ . Furthermore, for smaller values of  $p_T$ , the cross sections for both direct and indirect leptons from a new heavy  $W$  lie below the distribution of electrons which results from the decay of a virtual  $W(83)$ . Precision vertex detection is unlikely to improve the situation. For highly energetic  $\tau$ 's, it will be extremely difficult to identify the kink in the observed track which would indicate a one-charged-prong decay.

Hence, we consider the non-leptonic decays of the  $\tau$ , focusing on  $\tau \rightarrow \pi\nu$  and  $\tau \rightarrow \rho\nu$ . These are also one-charged-prong decays and so are unlikely to be found via vertex detection. However, the signal of a highly energetic isolated  $\pi$  or  $\rho$  in an otherwise quiet event makes such a signature viable. The  $\rho$  would be differentiated from the  $\pi$  by detecting the photons from the decay  $\rho^+ \rightarrow \pi^+ \pi^0$ ,  $\pi^0 \rightarrow \gamma\gamma$ . We shall proceed as if the detection of isolated  $\pi$ 's and  $\rho$ 's is 100% efficient. Clearly this will not be the case; further study is required to determine how feasible this approach can be.

In order to derive the spectrum of outgoing  $\pi$ 's and  $\rho$ 's arising from the sequential decay  $W \rightarrow \tau N$ ,  $\tau \rightarrow (\pi \text{ or } \rho) + \nu$ , we use an equation analogous to eq. 2.8. We therefore need to compute<sup>51</sup>  $ds/dE d\cos\theta$  for the process  $q\bar{q} \rightarrow W_{R,L} \rightarrow a + X$  (in the  $q\bar{q}$  center-of-mass frame) where  $a = \pi$  or  $\rho$  arises from  $W_{R,L} \rightarrow \tau N$ ,  $\tau \rightarrow a + \nu$ . It turns out that this quantity is proportional to the differential decay rate for helicity  $\lambda = \pm 1/2$   $\tau$ 's,  $d\Gamma/dE_\rho$ , computed in the same coordinate frame (i.e. the  $W$  rest frame where the  $\tau$  is moving). We present here a derivation of this decay rate,<sup>53</sup> the reader who wishes to skip the details may immediately proceed to the final result given in eq. 4.14.

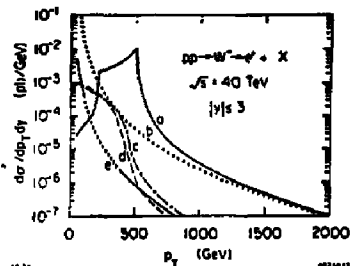


Fig. 11. Single  $e^+$   $p_T$ -spectra at  $\sqrt{s} = 40$  TeV from the decay of a charged vector boson. We show distributions of  $e^+$  from direct decays  $W \rightarrow eN$  and from the sequential decay  $W^+ \rightarrow \tau^+ \rightarrow e^+$ . The curves correspond to (a)  $W^+(1000) \rightarrow e^+$ ; (b)  $W^+(83) \rightarrow e^+$ ; (c)  $W_L(1000) \rightarrow \tau^+ \rightarrow e^+$ ; (d)  $W_R(1000) \rightarrow \tau^+ \rightarrow e^+$ ; and (e)  $W^+(83) \rightarrow \tau^+ \rightarrow e^+$ . The mass of the new  $W$  is taken to be 1 TeV.

We begin by noting that in the rest frame of the  $r$ , the four-momentum of particle  $a$  is given by:

$$k_a = \left( \frac{m_r^2 + m_a^2}{2m_r} ; \left( \frac{m_r^2 - m_a^2}{2m_r} \right) \sin \theta , 0 , \left( \frac{m_r^2 - m_a^2}{2m_r} \right) \cos \theta \right) \quad (4.7)$$

where  $\theta$  is the angle of particle  $a$  with respect to the incoming quark. We now consider the decay  $\tau \rightarrow s + \nu$  in the  $q\bar{q}$  rest frame, where the  $\tau$  is moving with velocity  $v$  which is nearly the speed of light (i.e.  $\sqrt{s} \gg m_\tau$ , where  $s$  is the squared center-of-mass energy for the scattering process). Denoting  $\gamma = (1 - v^2)^{-1/2} \gg 1$ , the energy  $E_a$  of particle  $a$ , in the  $q\bar{q}$  rest frame is:

$$E_0 \approx \frac{1}{m_r} \left( m_r^2 \cos^2 \frac{\theta}{2} + m_s^2 \sin^2 \frac{\theta}{2} \right) \quad (4.8)$$

In the same frame, the energy of the  $\tau$  is  $E_\tau = \gamma m$ , so that the energy fraction is given by

$$z \equiv \frac{E_4}{E_1} \approx \frac{m_4^2}{m_1^2} + \left(1 - \frac{m_4^2}{m_1^2}\right) \cos^2 \frac{\theta}{2} \quad (4.9)$$

Thus, if we compute the decay angular distribution of particle  $a$  in the rest frame of the  $\tau$ , we will know using eq. 4.9 the energy distribution  $d\Gamma/dE_a$  of particle  $a$  in the  $q\bar{q}$  center-of-mass frame.

To compute the decay rate for  $\tau \rightarrow \mu\nu$ , we may take the  $\tau\mu\nu$  coupling to be given by  $(G_F g_F/\sqrt{2})\tau^\mu(1 - \gamma_5)$  as suggested by vector meson dominance. A straightforward computation leads to:

$$E_p E_r \frac{d\Gamma}{d^3 k_p} = \frac{G_F^2 g_F^2}{8\pi^2 m_p^2} \delta(m_r^2 - 2p_r \cdot k_p + m_p^2) \times [(m_r^2 - m_p^2)(m_r^2 + 2m_p^2) - m_r(m_r^2 - 2m_p^2)k_r \cdot k_p] \quad (4.10)$$

where  $k_\mu$  and  $p_\mu$  are the four-momenta of the  $\rho$  and  $\tau$  and  $s_\mu$  is the spin four-vector of the  $\tau$ . In the limit where  $m_\tau \ll m_\rho$ , the  $\tau$  emitted from a  $W_L$  ( $W_R$ ) will be purely left (right) handed

with helicity  $\lambda = -1/2$  ( $\lambda = +1/2$ ). In either case,

$$e_4 \cdot k_p = \frac{\lambda(m_e^2 - m_p^2) \cos \theta}{m_p} \quad (4.11)$$

where  $\theta$  is the angle between the spin vector and the  $p$ -momentum. (Note that by boosting the  $r$  along the direction of its spin, we can relate the angle  $\theta$  to the  $p$ -energy fraction  $z$  as given by eq. 4.9.) Plugging eq. 4.11 into eq. 4.10 and integrating over the energy of the  $p$ , using up the  $\delta$ -function, we obtain

$$\frac{d\Gamma}{d \cos \theta} = \frac{B_p \Gamma_p}{m_1^2 + 2m_p^2} \times \begin{cases} m_1^2 \cos^2 \frac{\theta}{2} + 2m_p^2 \sin^2 \frac{\theta}{2}, & \lambda = +\frac{1}{2} \\ m_1^2 \sin^2 \frac{\theta}{2} + 2m_p^2 \cos^2 \frac{\theta}{2}, & \lambda = -\frac{1}{2} \end{cases} \quad (4.12)$$

where  $B_s \equiv BR(\tau \rightarrow \mu\nu)$  and

$$B_p \Gamma_p = \frac{G_F^2}{16\pi} \left( \frac{g_p}{m_p} \right)^2 \frac{(m_e^2 - m_p^2)^2 (m_e^2 + 2m_p^2)}{m_e^2} \quad (4.13)$$

(Note that  $g_s$  has units of mass squared; its value can be deduced from the experimental value of  $B_p \Gamma_p$ .) Finally, using eq. 4.9 we may convert the  $d\Gamma/d\cos\theta$  given in eq. 4.12 into the differential  $\pi$  decay rate  $d\Gamma/dE_\pi$  in the  $q\bar{q}$  center-of-mass frame. The result is:

$$\left( \frac{d\Gamma}{dE_p} \right)_{\text{at real frame}} = \frac{4m_t^2 B_p \Gamma_p}{\sqrt{6} (m_t^2 - m_p^2)^2 (m_t^2 + 2m_p^2)}$$

$$\times \begin{cases} m_\rho^2[m_\rho^2 + \varepsilon(m_\rho^2 - 2m_\rho^2)] & \lambda = +\frac{1}{2} \\ 2m_\rho^2(m_\rho^2 - m_\rho^2) + (1 - \varepsilon)m_\rho^2(m_\rho^2 - 2m_\rho^2) & \lambda = -\frac{1}{2} \end{cases} \quad (4.14)$$

where, in the  $q\bar{q}$  rest frame,  $x = 2E_p/\sqrt{s}$ , in the approximation that  $m_s \ll \sqrt{s}$ . From eq. 4.8, we see that  $m_s^2/m_q^2 \leq x \leq 1$ . Equation 4.14 illustrates the general result that the energy distribution of the final state  $\rho$  reflects the polarization of the  $s$  which in turn reveals the nature of the  $W\bar{N}\gamma$  coupling.

The precise formula for  $d\sigma/dE \cos\theta$  (in the  $q\bar{q}$  center-of-mass frame) for the process  $q\bar{q} \rightarrow W_{L,R}^{\pm} \rightarrow \tau^{\pm} N, \tau^{\pm} \rightarrow \rho^{\pm} + \nu$  is derived in a separate contribution to these proceedings.<sup>51</sup> We quote the final result (valid for  $m_{\tau} \ll \sqrt{s}$ ):

$$\frac{ds}{dE_p d\cos\theta_p} = \frac{G_F^2 m_W^4 s (1 + \cos\theta_p)^2}{48\pi [(m_W^2 - s)^2 + \Gamma_W^2 m_W^2]} \frac{1}{\Gamma_p} \left( \frac{d\Gamma}{dE_p} \right)_{\text{pp rest frame}} \quad (4.15)$$

where  $\theta_p$  is the angle between the  $p$  and the incident quark direction. We have assumed that both the  $Wq\bar{q}$  and the  $WN\tau$  vertices are either both  $V-A$  or pure  $V+A$ . The  $p$  angular distribution cannot distinguish between these two cases.

The above computation can be repeated for  $r \rightarrow \pi\nu$ . Using a  $\pi\nu$  vertex of  $(G_F/\sqrt{2})f_\pi\gamma_5(1-\gamma_5)h_\nu^*$ , we find that all the results derived above are identical with the replacement  $m_\rho \rightarrow m_\pi$  and  $\rho/\rho_0 \rightarrow f_\pi$ . It is a good approximation to take  $m_\pi = 0$ ; then eq. 4.14 reads

$$\left( \frac{d\Gamma}{dE_\pi} \right)_{\pi \text{ and } \text{from}} = \frac{4B_0 \Gamma_\pi}{\sqrt{s}} \times \begin{cases} z, & \lambda = +\frac{1}{2} \\ 1-z, & \lambda = -\frac{1}{2} \end{cases} \quad (4.16)$$

This result has a simple physical interpretation. The  $\tau^-$  is either left or right-handed depending on whether it came from

$W_L$  or  $W_R$ . But the  $\nu_\tau$  is always left-handed. Thus, because the  $\tau$  is spinless, conservation of angular momentum implies that  $\tau$  is emitted preferentially "forward" in the case of  $W_R$  decay and "backward" in the case of  $W_L$  decay. This is illustrated in Fig. 12. In the  $\tau\bar{\nu}$  center-of-mass frame, this corresponds to an energy spectrum of the  $\tau$  which is harder (peaked at  $z = 1$ ) in  $W_R$  decay and softer (peaked at  $z = 0$ ) in  $W_L$  decay. The arguments above have been made for a  $\tau^+$  emitted from a negatively charged  $W$ . We can repeat the arguments for the case of the sequential decay  $W^+ \rightarrow \tau^+ \rightarrow \pi^+$  (or  $\rho^+$ ). The resulting energy distributions (eq. 4.14 and 4.16) are exactly the same. This can be checked by applying helicity arguments similar to the ones we have just made. Therefore, one need not measure the charge of the final state  $\tau$  or  $\rho$  in order to see a difference between  $W_L$  and  $W_R$ .

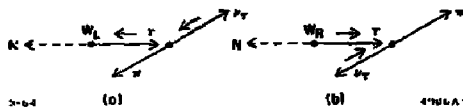


Fig. 12. Schematic view of the sequential decay  $W_{L,R} \rightarrow \tau N, \tau \rightarrow \pi \nu_\tau$ . The arrows above the  $\tau$  and  $\nu_\tau$  denote helicity. The  $\nu_\tau$  is always left-handed; the  $\tau$  helicity depends on the nature of the  $W$  as shown. Angular momentum conservation demands that the configurations shown above are the ones favored.

Before using these results, it is interesting to apply the physical interpretation just discussed to the case of sequential  $W \rightarrow \tau \rightarrow \rho$  decay. We have noted the close relation between the  $\pi$  and  $\rho$  formulas (eqs. 4.14 and 4.16). In particular, setting  $m_\rho = 0$  in eq. 4.14 leads to a result identical in structure to the  $\pi$  formula (eq. 4.16). Based on the analysis just discussed, this must imply that in the limit  $m_\rho \rightarrow 0$ , longitudinal  $\rho$ 's dominate. This is correct as can be observed from eq. 4.12. Using

$$\Gamma(\tau^-(\pm 1/2) \rightarrow \rho^-(\lambda) + \nu_\tau) \propto |d_{\pm 1/2, \lambda+1/2}^{1/2}(0)|^2 \quad (4.17)$$

(since the  $\nu_\tau$  necessarily has helicity  $-1/2$ ), we immediately see from eq. 4.12 that the  $d\sigma/dp_T$  rate for helicity  $-1$   $\rho$ 's is proportional to  $m_\rho^2$ . Thus, in the limit  $m_\rho \rightarrow 0$ , only the helicity zero  $\rho$ 's survive as claimed above (we cannot produce  $\lambda = +1$   $\rho$ 's due to angular momentum conservation). This may appear peculiar since we are used to thinking that massless vector particles are purely transverse. However, one must recall that a theory of massive vector bosons does not necessarily have a smooth limit to the massless theory. The longitudinal polarisation vector for the  $\rho$  is approximately  $e^L \approx k_\rho^L/m_\rho$  ( $\gamma, m_\rho \rightarrow 0$ ). The matrix element for  $\tau^- \rightarrow \rho^- \nu_\tau$  is  $j_\mu e^L$  where  $j_\mu = \bar{u}_\nu e^\mu [(1 - \gamma_5)/2] u_\nu$ . The  $m_\rho \rightarrow 0$  limit is not smooth as long as  $k_\rho^L j_\mu \neq 0$  which is the case here.<sup>54</sup> Thus, instead of decoupling, the longitudinal  $\rho$ 's dominate in this limit as we have observed above.

We may insert eq. 4.16 into eq. 2.8 to obtain the predicted spectrum of  $\rho$ 's (and  $\pi$ 's) from sequential  $W \rightarrow \tau N$  decay. A number of distributions have been given by Gunion and Haber in a separate contribution to the proceedings.<sup>55</sup> We provide some additional results here in Figs. 13 and 14.

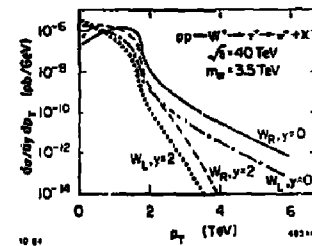


Fig. 13. Single  $\pi^+$   $p_T$ -spectra at  $\sqrt{s} = 40$  TeV from the sequential decay  $W^+ \rightarrow \tau^+ \rightarrow \pi^+$ . The  $W$  mass is taken to be 3.5 TeV. We show distributions for  $W_L$  and  $W_R$  for two fixed values of rapidity,  $y = 0$  and 2.

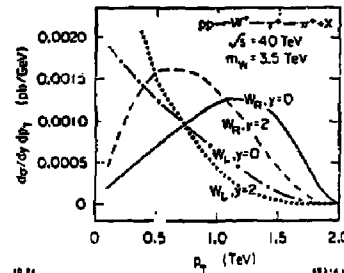


Fig. 14. Single  $\pi^+$   $p_T$ -spectra at  $\sqrt{s} = 40$  TeV from the sequential decay  $W^+ \rightarrow \tau^+ \rightarrow \pi^+$ . We have replotted Fig. 13 on a linear scale in order to focus on the  $p_T$ -region below 2 TeV.

As in the case of asymmetries discussed in the previous section, the minimum amount of data needed to discover a new  $W$  or  $Z$  is not sufficient to obtain information regarding its couplings. One could then ask - what is the heaviest charged  $W$  for which the observation of the sequential decay  $W \rightarrow \tau \rightarrow \pi$  can distinguish between  $W_L$  and  $W_R$ ? Gunion and Haber made an initial estimate and concluded that, assuming 100% efficiency for detection of pions, new  $W$  masses up to about 3.5 TeV allow for separation of  $W_L$  from  $W_R$ . A more realistic number awaits further experimental input as to the  $\tau$  detection efficiency.

One can imagine looking for three prong decays of the  $\tau$ . In this case, precision vertex detection could be of use if the three charged tracks can be individually identified. Finally, we note that the discussion above can also be applied to  $Z$  decays. Here, because the process of interest is  $Z^0 \rightarrow \tau^+ \tau^-$  followed by two  $\tau$ -decays, the formalism is more involved and needs to be more fully developed.

#### D. Horizontal Gauge Bosons at the SSC

One can consider gauge bosons which are not simply clones of the  $W(83)$  and the  $Z(94)$ . In this section, we will examine the possibility of observing horizontal gauge bosons at the SSC. Unlike the  $W(83)$ ,  $Z(94)$  and the new  $W$ 's and  $Z$ 's considered thus far, horizontal gauge bosons do not couple universally to

the different generations of fermions. For example, one can construct a model of horizontal symmetries, i.e. symmetries which relate fermions of different generations.<sup>31,32</sup> By gauging such a symmetry, one obtains horizontal gauge bosons. Such a theory represents one attempt to explain the replication of generations.

If such a scenario actually occurs, then a crucial parameter of the model is the mass scale which characterizes the horizontal symmetry breaking. A lower bound to such a mass scale can be obtained by considering current experimental limits on flavor-changing neutral currents (FCNC's). If horizontal gauge bosons,  $V_H$ , existed one would expect such bosons to mediate flavor-changing transitions. The nonobservation of certain FCNC's is then interpreted as a lower bound on the mass of  $V_H$ . Two stringent examples mentioned in Section 1D are the nonobservation of  $K_L \rightarrow \mu e$  and  $K^\pm \rightarrow \pi^\pm \mu e$ . Such processes could occur if  $V_H d\bar{s}$  and  $V_H s\bar{e}$  vertices existed in the theory. One typically finds<sup>32</sup> that  $M_H \gtrsim 5 - 100$  TeV depending on which FCNC reaction is used. This limit, however, depends on setting unknown mixing angles to unity and taking the horizontal and weak gauge couplings to be equal. Clearly, there is room to maneuver here - the horizontal bosons could be fairly light if appropriate mixing angles are small.

We may then consider the possibility of actual production and detection of  $V_H$  at the SSC. Roughly, one might expect to be sensitive to such bosons up to 10 TeV (similar to the case of a new  $W$ ). Suppose a horizontal boson exists which couples both to  $d\bar{s}$  and  $e\bar{\mu}$ . Then, one could produce such bosons by the Drell-Yan process - annihilating  $d\bar{s}$  to produce a physical  $V_H$  which subsequently can decay into  $e\bar{\mu}$ . The production cross sections are similar to that of new  $W$  production (since the probability of finding  $s$  or  $\bar{d}$  in the proton is similar). Albright, et.al. have obtained some predictions for  $V_H$  production cross sections based on various assumptions on the  $V_H$  mass and couplings. Details are presented in a separate contribution to these proceedings.<sup>33</sup> The process  $d\bar{s} \rightarrow e\bar{\mu}$  would be quite spectacular: a very quiet event except for a highly energetic back-to-back  $e\bar{\mu}$  pair. Clearly, such a signal would be nearly background free and one could claim evidence of new physics based on a handful of events.

However, the example we have chosen ( $d\bar{s} \rightarrow e\bar{\mu}$ ) is not the appropriate one. Given that the rare  $K$ -decays previously mentioned have not been observed, we know that a  $V_H$  which couples to both  $d\bar{s}$  and  $e\bar{\mu}$  must either be extremely heavy ( $\gtrsim 20$  TeV) or very weakly coupled. In the former case, the SSC energy is not large enough to produce such a  $V_H$ . In the latter case, the  $V_H$  can be produced, but due to the weak couplings, the production cross-section for  $V_H$  is too small. Either way, such a  $V_H$  cannot be seen at the SSC. These dismal conclusions have been reached solely because the FCNC constraints in  $K$ -decay are so severe. This is no longer the case in other systems. For example, very few restrictions are known regarding the transitions:

$$e\bar{u} \rightarrow \mu e, \tau e, \nu \mu \quad (4.18a)$$

$$d\bar{s} \rightarrow \mu \bar{s}, \tau \bar{s} \quad (4.18b)$$

If one takes the attitude that the non-existence of  $d\bar{s} \rightarrow e\bar{\mu}$  need not affect all other possible FCNC's, then one has the possibility of finding much lighter horizontal gauge bosons than previously envisioned. It is not entirely unreasonable that the third generation may be special (compared to the first two) in some way, allowing for the possibility that FCNC's involving at least one

third generation fermion could be substantially less suppressed than other FCNC's. Looking over the list in eq. 4.18, the  $\tau$ -lepton prominently stands out. Thus, efficient detection of  $\tau$ -leptons is highly desirable. In the previous section, we saw that one advantage of  $\tau$ -lepton detection is that it can provide information on the vector boson couplings. In the present context, a further advantage is revealed. The  $\tau$ -lepton may provide a window to new physics beyond the Standard Model. Once again, the signature of  $V_H$  production via the processes listed in eq. 4.18 is quite clean, and only a few events are needed to signal something new. Discovery limits for horizontal gauge bosons found by Albright, et.al., are presented in Table 5. In obtaining these numbers, all unknown mixing angles have been set to unity. The unknown horizontal gauge boson coupling  $\alpha_H = g_H^2/4\pi$  has been set to either 1, 0.1 or  $\alpha_H = g_W^2/4\pi$ . These assumptions are quite arbitrary so the results in Table 5 should be considered only as illustrative.

Table 5

Process	Discovery Limit		
	$\alpha_H = 1.0$	$\alpha_H = 0.1$	$\alpha_H = \alpha_W$
$d\bar{s} + u\bar{c} \rightarrow e^- \mu^+$	33	15	11
$d\bar{b} + u\bar{l} \rightarrow e^- \tau^+$	25	12	9
$s\bar{b} + c\bar{l} \rightarrow \mu^- \tau^+$	16	7	5
$d\bar{d} + s\bar{b} + u\bar{d} + c\bar{l} \rightarrow e^- \mu^+ + \mu^- \tau^+$	30	17	12

Table 5: Discovery Limits of Horizontal Gauge Boson masses at the SSC with  $\sqrt{s} = 40$  TeV and  $\mathcal{L} = 10^{33} \text{ cm}^{-2} \text{ sec}^{-1}$ . All masses are given in TeV. The horizontal gauge boson coupling is chosen to have one of three possible values, where  $\alpha_H = \alpha/\sin^2 \theta_W \approx 0.03$ . Unknown mixing angles have been set equal to unity. The criterion for discovery is the observation of five events in one year ( $10^7$  sec) of running.

Therefore, the SSC will significantly extend the lower limits for the masses of hypothesized horizontal gauge bosons, or equivalently will be able to set more stringent limits on FCNC transitions such as those listed in eq. (4.18). Such limits can complement other techniques which may be used at the SSC to study the possible existence of FCNC. For example, due to large number of  $b$ -quarks expected at the SSC<sup>34</sup> (approximately  $10^{12}$  per year will be produced for a machine with  $\mathcal{L} = 10^{33} \text{ cm}^{-2} \text{ sec}^{-1}$ ), one can search for rare decays of the  $B^0$ -meson. Thus, the transition  $b\bar{d} \rightarrow \mu e$  might be detected either by a rare  $B^0$  decay or by the production of a horizontal gauge boson. To compare the sensitivity of both processes, we may make the following estimate:

$$BR(B^0 \rightarrow \mu e) \sim \frac{g_H^2 m_W^4}{9\pi M_{V_H}^2} \frac{m_\mu^6}{m_\mu^2 \tau_\mu} \quad (4.19)$$

where the ratio of lifetimes is  $\tau_b/\tau_\mu \approx 5 \times 10^{-7}$ . In the formula above, we have set the unknown horizontal gauge boson mixing angle to unity. As an example, if we choose  $g_H = g_W$ , we would find from Table 5 that horizontal gauge bosons with  $M_{V_H} \lesssim 9$  TeV can be detected directly; the corresponding sensitivity given by eq. 4.19 is  $BR(B^0 \rightarrow \mu e) \gtrsim 10^{-6}$ . Whether such branching ratio could be detected at the SSC remains to be seen.

As we mentioned in Section 1D, other schemes exist which predict gauge bosons which do not couple universally to the generations. A model of Holdom<sup>35</sup> has inspired us to consider

the possibility of a gauge boson  $Y$  which prefers to decay into heavy quarks or leptons, or into  $W$ -pairs. As this is also what one expects from a heavy Higgs scalar, it is of interest to consider how a vector and a scalar particle with such properties could be distinguished. Kaiser has considered this problem in detail and I present here his analysis verbatim.

If the  $Y$  is produced in  $pp$  or  $pp$  collisions via gluon fusion and heavy quark loops, it will tend to have helicity  $\lambda = \pm 1$ , rather than  $\lambda = 0$ . Now, suppose  $Y \rightarrow f\bar{f}$ , where  $f$  is a quark or lepton, with a coupling of the form

$$\epsilon_\mu u_f \gamma^\mu (a + b \gamma_5) v_f . \quad (4.20)$$

Here  $\epsilon_\mu$  is the  $Y$  polarization vector. Assume that  $|\lambda(Y)| = 1$ , and that the  $Y$  may have a polarization

$$P \equiv \frac{N(\lambda = +1) - N(\lambda = -1)}{N(\lambda = +1) + N(\lambda = -1)} . \quad (4.21)$$

Then, the angular distribution of  $f$  in the  $Y$  rest frame with respect to the  $Y$  direction of motion in the lab is

$$\frac{d\Gamma}{d(\cos\theta)} \propto 2|\alpha|^2 m_f^2 + (|\alpha|^2 + |\delta|^2) \vec{p}^2 (1 + \cos^2\theta) - P(ab^* + a^*b)m_f |\vec{p}| \cos\theta . \quad (4.22)$$

Here  $m_f$  and  $m_Y$  are the  $f$  and  $Y$  masses, and  $|\vec{p}|$  is the  $f$  momentum in the  $Y$  rest frame. Note that as long as  $\vec{p}^2/m_f^2$  is not small, this angular distribution is very different from the isotropy that would characterize a Higgs decay.

Now suppose  $Y \rightarrow W^+ W^-$ . In principle, there are 7 possible couplings among three  $J = 1$  particles. To illustrate the decay angular distributions which one may expect, we take the  $YWW$  coupling to have the same form as the  $Z^0WW$  or  $\gamma WW$  gauge coupling in the standard model. Assuming again that  $|\lambda(Y)| = 1$ , we find for the  $W^+$  distribution in the  $Y$  rest frame

$$\frac{d\Gamma}{d(\cos\theta)} \propto 1 + \left( \frac{r^2 - 4r + 12}{16r} \right) \sin^2\theta , \quad (4.23)$$

where  $r = m_f^2/m_Y^2$ . The coefficient of  $\sin^2\theta$  grows monotonically from  $3/16$  at  $r = 4$  (threshold) to infinity at  $r = \infty$ . For, say,  $m_f = 5m_Y$ , it is already 1.34. Thus, as in the decay to fermions, the angular distribution differs substantially from isotropy.

Note that the angular distribution, eq. (4.23), does not depend on the polarization  $P$  (eq. (4.21)) of the  $Y$ . Thus, this distribution should be the same as that for  $e^+e^- \rightarrow W^+W^-$  via an  $s$ -channel  $Z^0$  pole, since the unpolarized beams produce an intermediate  $Z^0$  with equal amounts of  $J_z = +1$  and  $J_z = -1$ , and no  $J_z = 0$  ( $s$  axis = beam axis). This claim is indeed correct as can be easily checked.<sup>37</sup>

### E. Implications of a Right-Handed Neutrino.

We have indicated in Section 1A that in  $SU(2)_L \times SU(2)_R \times U(1)$  models, one necessarily has to introduce a right-handed neutrino field  $N$  into the theory. The properties of the  $N$  field are not well constrained; a recent discussion of the relevant constraints has been given by Gronau, Leung and Rosner.<sup>38</sup> In particular, these authors point out that the experimental limits on the  $N$  mass and its mixing with ordinary neutrinos are rather poor for  $m_N \geq 1$  GeV.

Our main interest regarding the  $N$  is how it may affect the observation of a new  $W_R$  whose leptonic decays are expected to be  $W_R \rightarrow eN$ . (Of course, the  $N$  is interesting in its own right; although this would take us beyond the scope of this report.) If one assumes that the  $N$  escapes all detectors as missing energy, then the signature of a  $W_R$  will be similar to that of the  $W$ (83). On the other hand, the  $N$  might decay inside the detector. In this case, there are two possibilities depending on whether a separate decay vertex for the  $N$  can be detected. In either case, one may no longer have a missing energy trigger to help select out events corresponding to new  $W$  production. Guinon and Kaiser<sup>39</sup> have carefully considered a separate contribution various scenarios for the production of new  $W$  bosons which decay into  $N$  in the cases of  $pp$  and  $sp$  collisions. We simply summarise some of the salient features here.

One can estimate the lifetime of the  $N$  which depends on a number of assumptions. For example, the  $N$  can decay via virtual  $W_R$  emission or through its mixing with the ordinary neutrinos. Assuming that the former is the dominant mechanism, we find:

$$\tau_N \approx 4 \times 10^{-11} \text{ sec} \left( \frac{5 \text{ GeV}}{m_N} \right)^3 \left( \frac{M_{W_R}}{1 \text{ TeV}} \right)^4 \quad (4.24)$$

This formula illustrates clearly that by adjustment of the relevant parameters, a lifetime consistent with each one of three possible scenarios mentioned above is possible. If we again neglect mixing effects, the  $N$  will decay via:

$$N_e \rightarrow e^\pm + 2 \text{ jets} \quad (4.25)$$

and similarly for the  $N$  associated with other lepton flavors. These modes have two noteworthy properties. Since  $N$  is likely to be a Majorana lepton, it will decay equally into  $e^+$  and  $e^-$ . This could be extremely distinctive, but requires the detector to be able to measure the electron charge (or the muon charge in  $N_\mu \rightarrow \mu^\pm + \text{jets}$ ). Furthermore, the electrons themselves may be hard to locate if they are buried inside one of the hadronic jets (however, this is not a problem for muons). Second, the process given in eq. 4.25 has the feature that there is no missing energy (as long as the jets do not consist of heavy quarks which semi-leptonically decay). Thus, one will have to trigger on a class of events consisting of one isolated lepton, a second lepton, hadron jets and very little missing transverse energy. Such a trigger is likely to make the new  $W$  search more complicated than the search for  $W$ (83). However, the isolated lepton exhibits a prominent Jacobian peak, and the remaining particles should reconstruct (roughly) to a unique mass.

For completeness, it is worthwhile to mention certain changes if the mixing of  $N$  with ordinary neutrinos dominates its decay. First, the  $N$  lifetime tends to be shorter, so probably no separated vertex will be observable. Second, in addition to the decay modes discussed above (eq. 4.25), there are completely leptonic modes which always involve at least one neutrino. Thus, in this case, the missing transverse energy trigger may be useful to isolate some of the  $W \rightarrow eN$  events.

### F. Directions for Future Investigations

We end this report with a list of unanswered questions which we believe should be addressed in future studies of new  $W/Z$  physics:

a) How clean are new  $W/Z$  signals under realistic experimental conditions? For example, in the discovery of the  $W(83)$ , an important feature in the detection of isolated electrons was checking that the  $e^-$  energy and momentum measurement matched. At the SSC, a momentum measurement becomes increasingly difficult as the electron momentum increases. Thus, it is likely that the above technique used to clean up the  $W(83)$  sample will not be available for new heavier  $W$ 's. Thus, an important question to answer is - with what efficiency can one identify isolated electrons at the SSC. (Some of these issues have been considered by Carr and Eichten in these proceedings.<sup>48</sup>)

b) What are the backgrounds to  $W_R - eN$  should the  $N$  decay be observable? We have speculated that the signal of  $W_R$  production is likely to remain clean even if the  $N$  decay products are observed. But this needs to be carefully checked. What are the other possible sources for  $e^+e^-$  + hadron jets plus negligible missing  $p_T$ ? Can one trigger effectively on such events at the SSC?

c) How efficiently can one detect  $\tau$ -leptons? Is it realistic to detect  $\tau$ 's by observing isolated  $\pi$ 's and/or  $\rho$ 's? What about the possibility of seeing a separated vertex and identifying it as a three-prong  $\tau$ -decay. Could such a signal be separated from charm production?

d) Calculations of distributions in  $Z^0 \rightarrow \tau^+\tau^-$  need to be worked out. A formalism should be developed by which one can use information from the distribution of  $\tau$  decay products to reconstruct the  $Z^0$  couplings to fermions.

e) The coupling of a new  $W$  to fermions can be partially obtained from asymmetry studies. If  $W \rightarrow eN$ , the  $N$  is not seen, then incomplete information exists on the kinematics of each event. More work is needed to determine whether one can still make use of the asymmetry in this case. Furthermore, the analysis given in this report has assumed that the missing  $N$  is massless. One needs to investigate possible effects that may arise if the  $N$  has non-negligible mass. How accurately can one infer the mass of the  $N$  if it escapes detection? If the  $N$  is seen, then the  $N$  decay products can provide additional clues to the nature of the  $W$  couplings (similar to the  $\tau$ -decay from  $W \rightarrow \tau N$ ).

f) In this report, we have focussed exclusively on leptonic decays of new  $W$ 's and  $Z$ 's. Can new gauge bosons be detected via their hadronic decay? Initial estimates indicate that this will be very difficult (perhaps impossible). Some progress, however, was made by the  $W$  ID group<sup>49</sup> which investigated the possibility of detecting the  $W(83)$  via its hadronic jets. Thus, the case for hadronic decays of new  $W$ 's and  $Z$ 's should be reopened and studied more carefully as progress is made on  $W(83)$  detection.

g) All cross section estimates for new  $W/Z$  production were based on the usual assumptions of the naive parton model. We have neglected primordial transverse momentum of initial state partons as well as transverse momentum due to QCD gluon radiation. In addition,  $K$ -factors and higher order QCD corrections have been neglected. It is worthwhile to investigate the effects of some of these neglected pieces. In particular, the transverse momentum spectrum

of new  $W$ 's and  $Z$ 's needs to be carefully taken into account. Apart from being an interesting exercise in QCD, to such effects will have observable consequences for the lepton spectra we have computed.

h) The implications of polarized hadron beams for new  $W/Z$  physics needs to be fully worked out. One would like to know how fully one can reconstruct  $W$  and  $Z$  couplings to fermions by observing the direct leptonic decays as a function of the beam polarisation. A side issue is the question of polarized structure functions. How reliable are the current methods for obtaining the polarised structure functions relevant for SSC energies?

I would hope that these questions could serve as a starting point for future work on new  $W/Z$  physics at the SSC, as well as providing an agenda for a New  $W/Z$  working group at the next SSC workshop.

#### Acknowledgements

I am grateful to the members of the New  $W/Z$  Physics subgroup whose hard work and perseverance made this summary report possible. In addition, I would like to thank Jack Gunion for his invaluable assistance in generating the curves shown in Figs. 6 - 11 and 13 - 14. Finally, conversations with Paul Langacker and Jon Rosner are gratefully acknowledged.

#### References and Footnotes

1. P. Langacker, R. W. Robinett, and J. L. Rosner, University of Chicago preprint EPI 84/12 (1984).
2. Short summaries of the work in Ref. 1 can be found in J. L. Rosner, P. Langacker and R. W. Robinett, *pp Options of the Supercollider*, p. 202, edited by J. A. Plichter and A. R. White, (1984); and in a contribution by the same authors to these Proceedings.
3. To avoid confusion, we shall denote the known massive gauge bosons by  $W(83)$  and  $Z(94)$  and use the generic notation  $W$  and  $Z$  for hypothetical charged and neutral gauge bosons which could be discovered at the SSC.
4. G. Arnison, et al. *Phys. Lett.* **122B**, 103 (1983); **126B**, 308 (1983); **129B**, 273 (1983); G. Banner, et al. *Phys. Lett.* **122B**, 476 (1983); P. Bagnulo, et al. *Phys. Lett.* **129B**, 130 (1983).
5. These arguments have been given in detail in many places. For example, see H. E. Haber and G. L. Kane, Michigan preprint UM HE TH 83-17 (1984) to be published in *Phys. Reports*.
6. E. Eichten, I. Hinchliffe, K. Lane and C. Quigg, FERMILAB PUB-84/17-T (1984).
7. P. Langacker, *Phys. Rep.* **72**, 185 (1981).
8. Two very useful reviews on left-right symmetry which contain a complete set of references are listed in Refs. 9 and 10.
9. R. N. Mohapatra, Lectures delivered at the NATO Summer School on Particle Physics, Sept 4 - 16: Munich, West Germany; Maryland preprint Md DP-PP-84-0012 (1984).

10. G. Senjanovic, in *Phenomenology of Unified Theories*, edited by H. Galic, B. Guberina and D. Tadic, p. 133 (World Scientific, Singapore, 1984).
11. For a recent review on Majorana neutrinos, see B. Kayser, to appear in *Comments on Nuclear and Particle Physics*.
12. This mechanism was first proposed by M. Gell-Mann, P. Ramond and R. Slansky, in *Supergavity*, edited by D. Freedman, et. al., (North Holland, Amsterdam, 1979) and independently by T. Yanagida, KEK Lectures (1979).
13. M. Grotz, C. N. Leung and J. L. Rosner, *Phys. Rev.* **D29**, 2539 (1984).
14. M. Kobayashi and T. Maskawa, *Prog. Theor. Phys.* **49**, 652 (1973).
15. J. Cronin, invited talk at the 1984 SLAC Summer Institute on Particle Physics, July 23 - Aug 3, 1984.
16. E. Fernandez, et al., *Phys. Rev. Lett.* **51**, 1022 (1983); N. S. Lockyer, et al., *Phys. Rev. Lett.* **51**, 1316 (1983).
17. H. Harari and M. Leurer, *Nucl. Phys.* **B223**, 221 (1984).
18. See, for example, W. J. Marciano, in *Proceedings of the International Symposium on Lepton and Photon Interactions at High Energies*, Cornell University, August 4 - 9, 1983, p. 80 edited by D. G. Casse and D. L. Kreinick.
19. T. G. Rizzo and G. Senjanovic, *Phys. Rev.* **D25**, 235 (1982); W. E. Caswell, J. Miltutinovic and G. Senjanovic, *Phys. Rev.* **D26**, 161 (1982); Y. Tosa, G. C. Branco and R. E. Marshak, *Phys. Rev.* **D26**, 1731 (1983); A. Sokorac, *Phys. Rev.* **D28**, 2320 (1983).
20. P. Langacker, Univ. of Penn. preprint UPR-0250T (1984).
21. F. I. Olness and M. E. Ebel, *Phys. Rev.* **D30**, 1034 (1984).
22. J. F. Donoghue and B. R. Holstein, *Phys. Lett.* **113B**, 382 (1982).
23. M. A. B. Beg, R. V. Budny, R. Mohapatra and A. Sirlin, *Phys. Rev. Lett.* **36**, 1252 (1977).
24. J. Carr, et al., *Phys. Rev. Lett.* **51**, 627 (1983).
25. G. Baur, M. Bander and A. Soni, *Phys. Rev. Lett.* **48**, 848 (1982).
26. F. J. Gilman and M. H. Reno, *Phys. Rev.* **D29**, 937 (1984).
27. R. Shrock, *Phys. Rev.* **D24**, 1232 and 1275 (1981).
28. Y. Aizawa, et al., *Phys. Lett.* **104B**, 84 (1981); R. Hayano, et al., *Phys. Rev. Lett.* **48**, 1305 (1982).
29. T. G. Rizzo and G. Senjanovic, *Phys. Rev.* **D24**, 704 (1981); V. Barger, E. Ma and K. Whisnant, *Phys. Rev.* **D26**, 2378 (1982); K. G. Deshpande and R. J. Johnson, *Phys. Rev.* **D27**, 1165 (1983).
30. We have used (in the notation of Ref. 7)

$$q_L^T \gamma^\mu q_L^T = -q_R^T C^{-1} \gamma^\mu C q_R^T = q_R^T \gamma^\mu q_R^T = -q_R \gamma^\mu q_R$$

which follows from the properties of the charged conjugation matrix  $C$ . The last equality follows from the fact that the fermion fields anticommute.

31. T. Masaoka and T. Yanagida, *Prog. Theor. Phys.* **60**, 822 (1978); **61**, 1434 (1979); P. Wilczek and A. Zee, *Phys. Rev. Lett.* **42**, 421 (1979); H. Georgi, *Nucl. Phys.* **B156**, 126 (1976); A. Davidson and K. C. Wali, *Phys. Rev.* **D21**, 787 (1980); *Phys. Rev. Lett.* **46**, 691 (1981).
32. R. N. Cahn and H. Harari, *Nucl. Phys.* **B126**, 135 (1980).
33. Particle Data Group, *Rev. Mod. Phys.* **56**, S1 (1984).
34. E. Farhi and L. Susskind, *Phys. Rev.* **D20**, 3404 (1979); S. Dimopoulos and L. Susskind, *Nucl. Phys.* **B155**, 237 (1979); E. Eichten and K. Lane, *Phys. Lett.* **90B**, 125 (1980).
35. B. Holdom, *Phys. Lett.* **143B**, 227 (1984).
36. R. L. Jaffe and J. R. Primack, *Nucl. Phys.* **B61**, 317 (1973); L. B. Okun and M. B. Voloshin, *Nucl. Phys.* **B120**, 461 (1977); C. Quigg, *Rev. Mod. Phys.* **54**, 297 (1977); R. P. Feynman, T. Trueman and L. L. Wang, *Phys. Rev.* **D16**, 1397 (1977); J. Kogut and J. Shigemitsu, *Nucl. Phys.* **B129**, 461 (1977); V. Barger, E. Ma and K. Whisnant, *Phys. Rev.* **D22**, 727 (1980); J. Ellis, M. K. Gaillard, G. Girardi and P. Sorba, *Ann. Rev. Nucl. Part. Sci.* **33**, 443 (1982); R. Hogan and M. Jacob, *Proceedings of CERN School of Physics*, Malente (PRG) 1980; CERN 81-04, p. 65.
37. R. M. Barnett, H. E. Haber and K. S. Lackner, *Phys. Rev. Lett.* **51**, 176 (1983) and *Phys. Rev.* **D29**, 1381 (1984).
38. See G. Arnison, et al., ref. 4; C. Rubbia, invited talk given at the 1984 SLAC Summer Institute for Particle Physics, July 23 - Aug 3, 1984.
39. For a review, see N. S. Craigie, K. Hidaka, M. Jacob and F. M. Renard, *Phys. Rep.* **92**, 69 (1983).
40. G. W. Lock and E. Fischbach, *Phys. Rev.* **D16**, 1369 (1977); K. H. Craig, *Nucl. Phys.* **B109**, 186 (1976); H. E. Haber and G. L. Kane, *Nucl. Phys.* **B145**, 109 (1978); F. E. Paige, T. L. Trueman and T. N. Tadros, *Phys. Rev.* **D19**, 935 (1979); J. Ranft and G. Ranft, *Nucl. Phys.* **B165**, 395 (1980); K. Hidaka, *Phys. Rev.* **D21**, 1316 (1980); *Nucl. Phys.* **B192**, 369 (1981); R. Kinnunen and J. Lindfors, *Nucl. Phys.* **B189**, 63 (1981).
41. R. Carlits and J. Kaur, *Phys. Rev. Lett.* **39**, 673 (1977); J. Kaur, *Nucl. Phys.* **B12B**, 219 (1977); F. Close and D. Sivers, *Phys. Rev. Lett.* **39**, 1116 (1977); J. Babcock, E. Monsey and D. Sivers, *Phys. Rev.* **D16**, 1483 (1977).
42. P. Chiappetta and J. Soffer, preprint CPT-84/P-1615 (1984).
43. Design Report: An Experiment at  $\bar{D}0$  to Study Anti-Proton Collisions at 2 TeV, Fermilab, December, 1983.
44. M. G. D. Gilchriese and H. H. Williams, "Tracking Detectors for Very High Energy Hadron-Hadron Collisions," in the Summary Report of the PSSC Discussion Group, edited by P. Hale and B. Wipstein, Fermilab publication (1984).
45. G. Gollin, in *pp Options for the Supercollider*, p. 226, edited by J. A. Pilcher and A. R. White, (1984).
46. S. D. Holmes and C. W. Leemann, "Electron Proton Collider at the SSC," these Proceedings.
47. J. F. Gunion, "Litzmus Tests for a Lepton Beam," these Proceedings.
48. J. F. Gunion and B. Kayser, "Searching for New  $W$ 's and Associated Neutrinos," these Proceedings.
49. J. F. Gunion, "Lepton Spectra and Discovery Limits for New Gauge Bosons," these Proceedings.

50. N. G. Deshpande, J. F. Gunion and H. E. Haber, "Reconstructing Couplings from Asymmetries in Heavy  $J$  Boson Decays," these Proceedings.
51. H. E. Haber, "Thus-A Probe of New  $W$  and  $Z$  Couplings," these Proceedings.
52. J. F. Gunion and H. E. Haber, " $\nu$ -Decay Spectra at the SSC," these Proceedings.
53. This method of derivation which follows was suggested by Fred Gilman.
54. We are grateful to Bill Bardeen for conversations on these points. Explicit calculations of the relevant helicity amplitudes have been performed by Boris Kayser; his results are in agreement with the above conclusions.
55. C. E. Albright, N. G. Deshpande, J. F. Gunion and H. E. Haber, "Search for Horizontal Gauge Bosons at the SSC."
56. G. L. Kane, invited talk at the Conference on the Physics of the XXI Century, Tucson, AZ, December 1983; Univ. of Michigan preprint UM TH 83-25 (1984).
57. See, for example, J. Ellis, in Proceedings of the 1978 SLAC Summer Institute on Particle Physics, edited by M. Zippf, p. 69 (SLAC Report No. 215, 1978).
58. J. Carr and E. Eichten, these Proceedings.
59. F. E. Paige, et al., " $W$ ,  $Z \rightarrow$  jets Identification," these Proceedings.
60. See, for example, G. Altarelli, R. K. Ellis, M. Greco and G. Martinelli, CERN preprint, Ref. TH. 3851 (1984) and reference contained therein.

## **DISCLAIMER**

This report was prepared as an account of work sponsored by an agency of the United States Government. Neither the United States Government nor any agency thereof, nor any of their employees, makes any warranty, express or implied, or assumes any legal liability or responsibility for the accuracy, completeness, or usefulness of any information, apparatus, product, or process disclosed, or represents that its use would not infringe privately owned rights. Reference herein to any specific commercial product, process, or service by trade name, trademark, manufacturer, or otherwise does not necessarily constitute or imply its endorsement, recommendation, or favoring by the United States Government or any agency thereof. The views and opinions of authors expressed herein do not necessarily state or reflect those of the United States Government or any agency thereof.

## **NOTICE**

**PORTIONS OF THIS REPORT ARE ILLEGIBLE**  
It has been reproduced from the best  
available copy to permit the broadest  
possible availability.